THE JOURNAL OF PHYSICAL CHEMISTRY B

Article

pubs.acs.org/JPCB

Phenomena Associated with Gel−Water Interfaces. Analyses and Alternatives to the Long-Range Ordered Water Hypothesis

J. Michael Schurr*

Department of Chemistry, University of Washington, Box 351700, Seattle, Washington 98195-1700, United States

ABSTRACT: Interfacial regions between certain gels and their surrounding solutions were observed by Pollack and co-workers to exhibit several unexpected phenomena: (1) long-range exclusion of charged microspheres out to typical distances of ∼100−200 μm from the gel surface; (2) significant electrostatic potentials extending over comparable distances; (3) a reduced intensity of upward spontaneous thermal IR emission over a region 300−500 μm wide at or near the gel−solution interface; and (4) a significantly lower proton T_2 and an apparently reduced H_2O self-diffusion coefficient over a zone ∼60 μm wide at or near the gel−solution interface in high resolution NMR imaging experiments. To account for such observations, they proposed that a region of long-range ordered water bearing a net negative charge, but lacking mobile charge carriers, extended ∼100−200 μm outward from the gel surface. In this paper, various problems associated with the ordered water hypothesis, including contradictions by experiments from many other laboratories, are briefly discussed, and testable alternative explanations for the observed phenomena are proposed. Exclusion zones are suggested to arise from chemotaxis of the microspheres in long-range diffusion gradients of OH^- (or H^+) and salt, the theory of which was developed and compared with the observations on non-ionic gels in a companion paper. The same theory together with the expected directions of ion transfers between gel and solution are now used to predict qualitatively the exclusion/attraction behavior of microspheres in the presence of ionic gels and ionomers. The electrostatic potentials are interpreted as long-range liquid-junction potentials arising from the same long-range diffusion gradients of OH^- (or H^+) and salt in the unstirred solutions of Pollack and co-workers. Alternative explanations in terms of plausible experimental artifacts are suggested for both the reduced intensity of IR thermal emission and the lower proton T_2 and apparent H_2O diffusion coefficient in the NMR imaging experiments.

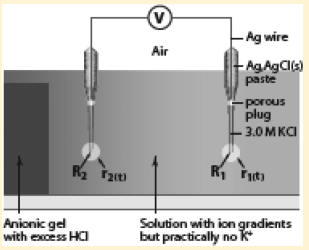

INTRODUCTION

A number of interesting phenomena in aqueous solutions near the surfaces of various hydrophilic gels and ionomers were observed and partially characterized by Pollack and co-workers.[1−10] The most extensive observations pertain to the motions of suspended microspheres in the surrounding solution, which commonly, but not always, moved outward from the surface of the gel to form an exclusion zone of width ∼50 to ∼600 μm, depending upon conditions.[1−9] Potential measurements using reversible microelectrochemical electrodes indicated a potential drop from values, ∼ −120 to −200 mV, at the surface of a negatively charged ionic gel or ionomer to nearly zero over a distance comparable to or somewhat larger than exclusion zone widths for such gels.[2,3,5,6] Infrared thermal emission images of a Nafion film either partially or entirely immersed in an aqueous solution exhibited a "dark" zone of ∼300−500 μm width at or near the edge of the film.[2] Finally, NMR T_2-imaging of the water protons in bulk water, bulk gel, and their mutual interfacial region were reported along with pulsed field-gradient spin echo studies of the translational diffusion of water parallel to the interface in those same three regions.[2] The results of each of these four different kinds of experiments were attributed to an extensive zone of "structured water" extending outward from the gel surface,[1] more precisely, "a physically distinct and less mobile phase of water that can coexist indefinitely with the contiguous solute-containing phases".[2,8] This "long-range water ordering"[10] was suggested to involve partial alignment of water molecules to form a "liquid crystalline structure"[10] that was further suggested to be "initiated through hydrogen bonding with the nucleating surface".[2,3] Moreover, the putative ordered water of the exclusion zone near a negatively charged gel was purported to possess a net negative charge,[2−4,7] and to be "largely free of mobile charge carriers",[2] so as to retain the net negative charge indefinitely.

There are a number of serious problems with the proposed interpretation of the experimental results in terms of long-range ordered water, some of which were discussed in detail in a previous paper (I, 10.1021/jp302587d).[11] The relevant problems include the following:

(1) It was never conclusively established whether the exclusion zone is an equilibrium phenomenon, as advocated by Pollack and co-workers, or instead is a long-lived non-equilibrium transient effect, as proposed in paper I (10.1021/jp302587d).[11]

(2) The possibility that long-range chemical gradients, such as a pH gradient, might be responsible for the exclusion zone was considered by Pollack and co-workers but was rejected for three reasons,[1] all of which were shown to be invalid in paper I (10.1021/jp302587d).

(3) Not all hydrophilic gel or ionomer surfaces exhibit exclusion zones. Table 1 provides a summary of the

Received: March 17, 2012
Revised: May 2, 2013
Published: May 8, 2013

Table 1. Observations of Exclusion or Attraction for Negatively and Positively Charged Microspheres from Various Gel Surfaces in Water[1,5,7,9]

				negative microspheres			positive microspheres		
gel	intrinsic charge[g]	initial counterion	pre-bath[h]	group	soln/pH[i]	expt.	group	soln/pH[i]	expt.
PVA[a]	none	none	diw[j]	$-COO^-$	NaOH/8–10[k]	excl	$-CNNH_3^+$	HCl/2.5–4[l]	excl
poly HEMA[b]	none	none	diw[j]	$-COO^-$	NaOH/8–10[k]	NR[m]	$-CNNH_3^+$	HCl/2.5–4[l]	excl
poly(acrylamide)	none	none	diw[j]	$-COO^-$	NaOH/8–10[k]	excl	$-CNNH_3^+$	HCl/2.5–4[l]	NR[m]
poly(acrylic acid)	neg	H^+	diw[j]	$-COO^-$	NaOH/8–l0[k]	excl	$-CNNH_3^+$	HCl/2.5–4[l]	excl
poly(acrylamide + MG)[c]	pos	Cl^-/OH^-	diw[j]	$-COO^-$	NaOH/8–10[k]	no excl	$-CNNH_3^+$	HCl/2.5–4[l]	NR[m]
agarose	neg[n]	H^+	diw[j]	$-COO^-$	NaOH/8–10[k]	NR[m]	$-CNNH_3^+$	HCl/2.5–4[l]	excl
Nafion[d]	neg	H^+	acid[o]	$-COO^-$	NaOH/8–10[k]	excl	$-CNNH_3^+$	HCl/2.5–4[l]	NR[m]
Nafion[d]	neg	H^+	acid[o]	$-OSO_3^-$	NaOH/8–10[q]	excl	$-CNNH_3^+$	HCl/2.5–4[l]	NR[m]
Nafion[d]	neg	H^+	diw[p]	$-OSO_3^-$	NaOH/8–10[q]	excl	$-CNNH_3^+$	HCl/2.5–4[l]	excl
cation exchange[e]	neg	H^+	acid[o]	$-OSO_3^-$	NaOH/8–10[k]	excl	$-CNNH_3^+$	HCl/2.5–4[l]	attr
cation exchange[e]	neg	H^+	acid[o]	$-OSO_3^-$	Im buff/7.0[r]	excl			
anion exchange[f]	pos	OH^-	base[s]	$-OSO_3^-$	NaOH/8–10[q]	attr	$-CNNH_3^+$	HCl/2.5–4[l]	excl
anion exchange[f]	pos	OH^-	base[s]	$-OSO_3^-$	Im buff/7.0[r]	excl			

[a]PVA = poly(vinyl alcohol). [b]poly HEMA = poly(hydroxyethyl methacrylate). [c]Copolymer of acrylamide and a vinyl derivative of malachite green. [d]Copolymer of tetrafluoroethylene and perfluoroethylene sulfonic acid. [e]Cross-linked divinylbenzene polystyrene backbone functionalized with $-SO_3^-$ groups. [f]Cross-linked divinylbenzene polystyrene backbone functionalized with $-(N^+)(CH_3)_3$ groups. [g]Sign of the intrinsic charge of ionized acidic or basic groups covalently linked to gel. [h]Bath with which gel was last fully equilibrated prior to experiment. [i]Main base or acid and pH of microsphere suspension before contacting gel. [j]After multiple rinses, gels were equilibrated with deionized water (diw) for 2 days. [k]The indicated pH range is inferred from Figure 6 of Zheng and Pollack using exclusion zone widths in their Figures 2, 4, 5, 7, and 9.[1] The cation is assumed to be Na^+ for discussion purposes. [l]The indicated pH range is inferred from Figure 6 using exclusion zone widths in Figures 4, 5, 7, 9, and 10 of Zheng and Pollack.[1] The anion is assumed to be Cl^- for discussion purposes. [m]An experimental result was not reported for these conditions. [n]Agarose has a low density of negative charges compared to other charged gels and Nafion. [o]Gel or Nafion was last equilibrated with strong acid by supplier. Subsequent washing/rinsing with diw in the Pollack lab (≤10 min) does not suffice to reach equilibrium. [p]Nafion 117 sheets were equilibrated with deionized water (diw) for 1 week in the Pollack lab. [q]The vendor did not know the pH of the sulfated microsphere suspension, which is here simply assumed to match that of the carboxylated microsphere suspension. [r]The imidazole buffer consists of imidazole, imidazolium ion, and Cl^- counterion. [s]Gel was last equilibrated with strong base by the supplier. Subsequent washing/rinsing with diw in the Pollack lab (≤10 min) does not suffice to reach equilibrium.

experimental conditions and results of the reported exclusion zone studies. Although polyacrylamide gels exclude both carboxylated and amidinated microspheres under their respective typical conditions, gels comprising copolymers of acrylamide and a vinyl derivative of malachite green (a cationic dye) do not exclude (and presumably also do not attract) negatively charged carboxylated microspheres.[1]

In the absence of buffer (the usual condition for observing exclusion zones), a (negatively charged) cation exchange gel excluded carboxylated microspheres but actually *attracted* positively charged amidinated microspheres.[4] These attracted spheres packed so tightly in well-defined layers that a significant degree of "crystalline" order prevailed therein. Also, in the absence of buffer, a (positively charged) anion exchange gel excluded amidinated microspheres but *attracted* negatively charged carboxylated microspheres.[4] Again, the attracted microspheres packed so tightly that significant "crystalline" order was visible within the well-defined layers. These exceptions contradict any mechanism that predicts universal exclusion from hydrophilic gel surfaces.

(4) The exclusion phenomenon depends strongly upon the difference in pH between the microsphere suspension and a non-ionic gel, and disappears entirely when their pH's match,[1] even under conditions when the microspheres remain fully charged, as discussed in paper I (10.1021/jp302587d).

(5) The purported exclusion of proteins from the surfaces of hydrophilic gels and biological tissues is contrast to numerous observations demonstrating macromolecular access to such surfaces, as noted in paper I (10.1021/jp302587d).

(6) The permeability to small ions and the viscosity of the solute-accessible water in 1.5% agar gels, which should be "ordered" according to Pollack's nucleation idea, are within experimental error identical to those of bulk water. This was demonstrated by immersing solute-free 1.5% agar gels in solutions of individual solutes, including NaCl, KCl, urea, glucose, sucrose, bovine serum albumin (BSA), and hemoglobin, and measuring the diffusion coefficient and equilibrium concentration of each solute inside its gel. After correcting the measured values for the fraction of the total gel volume accessible to the solute ($\phi < 1.0$), and for the obstructive effects of the gel, the concentrations and diffusion coefficients in the gel were within experimental error identical to those in bulk solution.[12] For the smaller solutes, the total corrections were less than ~2–3.3%. This was discussed in detail in paper I (10.1021/jp302587d).

(7) Soluble proteins, lipid vesicles, and charged polystyrene latex spheres manifest no thick layer of bound water in their translational and rotational diffusion coefficients, as described in paper I (10.1021/jp302587d). Highly accurate diffusion coefficients computed for the crystal structures of 41 soluble proteins plus a layer of uniform thickness, 1.1 Å, which is much less than a water monolayer (3.0 Å), agreed with the respective experimental data well within experimental errors.[13]

(8) Unequivocal evidence that the structure of water in the exclusion zone differs from that of bulk water is lacking.

(a) Any significant difference in density should be manifested by a significant difference in refractive index. That in turn should produce visible halos extending out 100–200 μm from the surface of any hydrophilic gel or biological tissue immersed

dx.doi.org/10.1021/jp302589y | J. Phys. Chem. B 2013, 117, 7653–7674

in water, when viewed by phase contrast microscopy. Although well-understood artifactual halos of $\lesssim 3$ μm extent routinely appear in reported phase-contrast images of such objects, halos of 100−200 extent have never been reported for either hydrophilic gels or biological tissues of any kind.

(b) Any difference in orientational order would likely be manifested by significant birefringence of the exclusion zone. Although efforts to image such birefringence in an artifact-free manner with high sensitivity and precision are still in progress, up to the present, no unequivocal evidence of significant birefringence of the exclusion zone has been obtained (Dr. Werner Kaminsky, personal communication).

(c) UV−vis spectra were taken at various distances from a Nafion surface that was "bonded to one of the vertical faces of a standard cuvette".[2,10] A peak at ∼270 nm with an absorbance ∼1.6 was observed for a narrow beam that was indicated to pass parallel to the Nafion surface at a distance of ∼200 μm, and was suggested to arise from ordered water.[2,10] This interpretation is almost certainly incorrect for the following reason. The reddest peaks in the electronic spectra of the gaseous, liquid, and ice forms of water lie at, respectively, 128,[14] 149,[15] and 143[16] nm. The transition energy changes by −1.37 eV upon going from the vapor to normal liquid and by +0.35 eV upon going from normal liquid to the less dense ice. If the peak at 270 nm is attributed to this same transition in ordered water, then the change in transition energy upon going from normal liquid water to "ordered water" would be −3.7 eV. A change of this magnitude in a transition energy upon going from one intermolecular environment to another is unprecedented. This change in transition energy exceeds by 2.7-fold that upon going from vapor to normal liquid water and exceeds by 10.5-fold (and a change in sign) that upon going from the normal liquid to ice. Because properties of the putative ordered water, such as density, viscosity, and self-diffusion coefficient, are far more similar (if not completely identical) to those of the normal liquid than to those of ice or vapor, the change in transition energy upon going from liquid water to ordered water would be expected to be even smaller than the change in going from liquid water to ice, rather than 10.5-fold larger. If not an experimental artifact, the 270 nm absorption peak is most likely that of a small-molecule contaminant diffusing out of the Nafion. A metal phthalate plasticizer would be a possibility. At present, this observed peak cannot be regarded as direct evidence of ordered water.

These rather serious problems with the equilibrium long-range ordered water hypothesis strongly suggest that the actual explanation for exclusion zone formation lies elsewhere.

The concentration of small ions (including H^+ or OH^-) in the microsphere exclusion experiments exceeded 10^{-6} M in every case, so the Debye screening length was generally $\lesssim 0.3$ μm. Hence, equilibrium electrostatic forces could not possibly have excluded charged microspheres over a distance of ∼100−200 μm or held them in an ordered array at a distance ≥ 16 μm.[4] Moreover, non-ionic (neutral) gels do not give rise to an equilibrium electrostatic potential but nonetheless exclude microspheres. Evidently, the observed microsphere exclusion is not driven primarily by equilibrium electrostatic forces.

Macromolecular Chemotaxis. A theory of non-equilibrium chemotactic forces on isolated macromolecules was developed in paper I (10.1021/jp302587d), and pertains to forces arising from concentration gradients of small cosolutes.[11] Of particular importance are univalent ionic cosolutes, such as OH^--containing bases (e.g., NaOH) or H^+-containing acids (e.g., HCl) and univalent dissociated salts (e.g., NaCl), which interact strongly with titratable acidic (or basic) groups on the surface of the macromolecule, which is here taken to be a microsphere. When modest gradients of such a base (NaOH) or a salt (NaCl) exist, the total chemotactic force on a macromolecule arises from (1) thermodynamic binding of the base to carboxyl (or other acid) groups on the microsphere surface and (2) the effects of electrolyte (S) to alter the equilibrium constant for base binding and to lower the electrostatic free energy of the charged microsphere. The electrolyte, S, consists of the univalent base plus univalent salt, so the total electrolyte concentration is $c_S = c_{OH-} + c_{salt}$, where $c_{OH-} = c_{NaOH}$ and c_{salt} are the concentrations of base and salt, respectively. The total predicted chemotactic force on a microsphere with M carboxyl plus carboxylate groups on its surface is directed along the gradient, which defines the x-axis, and is given by

$$F_{ch} = kTMf[(\partial \ln c_{OH^-}/\partial x)_{T,P,c_P^\infty,c_{salt}} + W(\partial \ln c_S/\partial x)_{T,P,c_P^\infty,\hat{c}_{OH^-}}] \quad (1)$$

where k is Boltzmann's constant, T is the absolute temperature, $f = K_b c_{OH^-}/(1 + K_b c_{OH^-})$ is the fraction of surface carboxyl groups that are ionized, K_b is the equilibrium constant for the NaOH binding reaction, P−COOH + OH^- + Na^+ → P−COO^- + Na^+ + H_2O, and $W = 2\{1 + \partial\Gamma_S(P(COO^-)_N)/\partial N + \Gamma_{1S}(P(COO^-)_N)\}$, where $\Gamma_S(P(COO^-)_N)$ is the electrostatic microsphere−electrolyte preferential interaction coefficient (PIC) due to (non-binding) electrostatic interactions for a species with $N = Mf$ charged carboxylate groups and $\Gamma_{1S}(P(COO^-)_N) = (1/N)\Gamma_S(P(COO^-)_N)$ is the electrostatic PIC per carboxylate group.[17] The first term in eq 1 represents the effect of NaOH binding, and the second represents the effect of electrolyte to alter K_b and lower the electrostatic free energy, and its corresponding force is denoted by F_S. In the subscripts on the derivatives, T and P denote constant temperature and pressure, c_P^∞ denotes a constant infinitely dilute concentration of microspheres, c_{salt} denotes constant salt concentration, and $\hat{c}_{OH^-}$ indicates that the value of c_{OH^-} is held constant in f, but not elsewhere, when c_{OH^-} in $c_S = c_{OH^-} + c_{salt}$ is varied. After the second term in eq 1 is decomposed into its separate contributions from variations in c_{salt} and c_{OH^-}, eq 1 can be rewritten as

$$F_{ch} = F_{OH^-} + F_{salt} \quad (2)$$

where

$$F_{OH^-} = kTMf\{1 + W(c_{OH^-}/(c_{OH^-} + c_{salt}))\}(\partial \ln c_{OH^-}/\partial x)_{T,P,c_P^\infty,c_{salt}} \quad (3)$$

is the total contribution of the OH^- gradient and

$$F_{salt} = kTMfW(c_{salt}/(c_{OH^-} + c_{salt}))(\partial \ln c_{salt}/\partial x)_{T,P,c_P^\infty,c_{OH^-}} \quad (4)$$

is the contribution of the salt gradient.

An analogous chemotactic force on a microsphere with M amine plus ammonium groups on its surface, when immersed in gradients of an electroneutral acid (HCl), and univalent salt is given by

$$F_{ch} = kTMf[(\partial \ln c_{H^+}/\partial x)_{T,P,c_P^\infty,c_{salt}} + W(\partial \ln c_S/\partial x)_{T,P,c_P^\infty,\hat{c}_{H^+}}] \quad (5)$$

dx.doi.org/10.1021/jp302589y | J. Phys. Chem. B 2013, 117, 7653−7674

wherein $c_{H^+} = c_{HCl}$ is the concentration of univalent acid, $f = K_a c_{H^+}/(1 + K_a c_{H^+})$ is the fraction of amine groups that have thermodynamically bound an HCl according to the reaction $P{-}NH_2 + H^+ + Cl^- \rightarrow PNH_3^+ + Cl^-$, K_a is the equilibrium constant for that reaction, $c_S = c_{H^+} + c_{salt}$, and $W = 2\{1 + \partial\Gamma_S(P(NH_3^+)_N)/\partial N + \Gamma_{1S}(P(NH_3^+)_N)\}$, where $\Gamma_S(P(NH_3^+)_N)$ is the electrostatic microsphere–electrolyte preferential interaction oefficient (PIC) due to (non-binding) electrostatic interactions for a species with $N = Mf$ charged ammonium groups and $\Gamma_{1S}(P(NH_3^+)_N) = (1/N)\Gamma_S(P(NH_3^+)_N)$ is the *electrostatic* PIC per ammonium group. The subscript, $\hat{c}_{H^+}$, indicates that the value of c_{H^+} in f, but not elsewhere, is held constant when c_S is varied. After decomposing the second term in eq 5 into its separate contributions from variations in c_{salt} and c_{H^+}, eq 5 can be expressed as

$$F_{ch} = F_{H^+} + F_{salt} \tag{6}$$

where

$$F_{H^+} = kTMf\{1 + W(c_{H^+}/(c_{H^+} + c_{salt}))\}$$
$$(\partial \ln c_{H^+}/\partial x)_{T,P,c_P^\infty,c_{salt}} \tag{7}$$

is the total contribution of the H^+ gradient and

$$F_{salt} = kTMfW(c_{salt}/(c_{H^+} + c_{salt}))(\partial \ln c_{salt}/\partial x)_{T,P,c_P^\infty,c_{OH^-}} \tag{8}$$

is the contribution of the salt gradient.

Expressions analogous to eqs 1–4 apply also to thermodynamic binding of NaOH to phosphoryl, sulfuryl, or silanol groups on a microsphere surface. Likewise, expressions 5–8 apply also to thermodynamic HCl binding to amidine or guanidine groups on a microsphere surface.

In general, evaluation of $\Gamma_S(P(COO^-)_N)$ or $\Gamma_S(P(NH_3^+)_N)$ requires solution of the non-linear Poisson–Boltzmann equation for a discretely charged microsphere embedded in the relevant milieu, but in any case, W must lie in the range $0 \leq W \leq 2.0$ and in the limit of low density of surface charges and/or high salt concentration, $W \simeq 0$.[11]

The microsphere velocity induced by the total chemotactic force (in the case of OH^- binding), which is manifested by a traction (force per unit area) at the microsphere–solution interface, can be written as

$$u = (2/3)kT\sigma f\lambda G/\eta = F_{ch}/\zeta \tag{9}$$

where $\sigma = M/4\pi R^2$ is the number of surface groups per unit area, λ is the hydrodynamic slip length at the microsphere–solution interface, η is the solution viscosity, $G = \{(\partial \ln c_{OH^-}/\partial x)_{T,P,c_P^\infty,c_{salt}} + W(\partial \ln c_S/\partial x)_{T,P,c_P^\infty,\hat{c}_{OH^-}}\}$ is the gradient factor, and $\zeta = (6\pi\eta R)(R/\lambda)$ is the friction factor (inverse mobility) associated with the traction force. Equation 9 shows that the induced velocity is proportional to the chemotactic force divided by a friction factor that exceeds the Stokes friction factor, $(6\pi\eta R)$, by the ratio R/λ which is very large compared to 1.0 for microspheres with $R \geq 1.0$ μm. Nevertheless, the very large surface densities (and numbers) of (non-ionized plus ionized) groups on typical microphores admit significant velocities on the 1 μm/s scale, as shown in paper I (10.1021/jp302587d). The induced velocity is independent of particle radius, provided that σ and λ remain constant.

It was noted in paper I (10.1021/jp302587d) that the theory embodied in eqs 1–9 accounts qualitatively for practically all observations of Pollack and co-workers pertaining to induced microsphere motions near the surfaces of non-ionic (uncharged) gels. With a single adjusted parameter, λ/A_1, where $A_1 = 1/\sigma$ is the area per surface group, it accounts quantitatively for many of those same observations, including the temporal trajectories of the microspheres. The optimal value of λ/A_1 is compatible with plausible values of A_1 and λ. One question addressed here is whether this same theory can account qualitatively for the diverse observations of Pollack and co-workers pertaining to induced microsphere motions near the surfaces of ionic (charged) gels and ionomers.

In paper I (10.1021/jp302587d), it was also noted that any solution with a gradient of $\ln c_{OH^-}$ and/or $\ln c_{salt}$ in contact with a small patch, δA, of a flat glass surface, which bears OH^--binding silanol groups, experiences a force in a direction opposite to that exerted by the solution on the patch. When the gradient is tangential to the patch, the traction, or force per unit area, exerted on the solution at the solution–glass interface is $F^{sol}/\delta A = -kT(f/A_1)G$. This traction acts to move solution (relative to the glass) toward the less basic and/or less salty end of the gradient. The solution velocity, v_x, relative to the glass was calculated for an open channel under hypothetical conditions, where f, A_1, λ, and G are independent of x. The resulting v_x is initially given by an expression identical to eq 9, except that the factor of 2/3 is replaced by −1, and the parameters f, A_1, and λ apply to flat glass, rather than to a microsphere surface. At later times in a channel of finite length, the fluid piles up at the acidic and/or less salty end, which leads to backflow in the top layer, and eventually to formation of one or more convection cells. Equations 1 and 3 are valid only when the OH^- or H^+ binding reaction proceeds sufficiently rapidly that the microsphere surface moving in the gradient remains nearly at equilibrium with its local surroundings at all times. For a group that binds OH^-, this condition is $\ln[c_{OH^-}(x + \tau u)/c_{OH^-}(x)] = \tau u\, d\ln c_{OH^-}/dx \lesssim 0.1$, where u is the microsphere velocity and $\tau = \tau_{diss} + \tau_{bind}$ is the sum of the mean times to dissociate an OH^- and to bind another OH^-.[11] This states that the motion of the sphere along the gradient in time τ should result in a change in $\ln c_{OH^-}$ of less than 0.1, which corresponds to a $\lesssim$10% change in the contribution of the binding reaction to its standard state chemical potential. Failure to meet this condition will result in smaller microsphere velocities than those predicted by eq 9.

Plan of the Paper. Each of the following four main sections (denoted I, II, III, and IV) contains an analysis of one of the four main types of evidence that has been invoked to support the ordered water hypothesis.[10] In each case, the experiments and results are first summarized, particular problems with the ordered water interpretations beyond those already noted are discussed, and a plausible and testable alternative interpretation is proposed and analyzed. The final fifth section contains brief concluding remarks.

I. Microsphere Exclusion/Attraction by Ionic Gels. Pollack and co-workers investigated exclusion/attraction phenomena near the surfaces of various ionic (charged) gels and ionomers.[1−5,7−9] Such gels possess intrinsic charges, which might or might not be titratable at experimental pH's, as well as compensating counterions, which were not always identified. In addition, the gel may initially contain some free electrolyte (acid, base, or salt) at a concentration that depends upon both the concentration, c_0, of intrinsic charges inside the gel and the concentration of electrolyte in the *prebath* with which the gel was fully *equilibrated* prior to its contact with the microsphere suspension. If c_0 and the composition of the prebath are either

known or can plausibly be assumed, then by using Donnan theory it is possible to reckon the initial concentrations of all ionic species and the initial concentration of free electrolyte (excluding the complement of counterions) in the gel. Donnan theory can also be used to estimate how much the free electrolyte concentration within a particular gel would increase or decrease, when it is placed in contact with an infinite solution of a different electrolyte concentration. However, because of the Donnan effect, the rate of transfer of free electrolyte cannot be treated by the simple diffusion theory used for non-ionic gels. In addition, ionic gels may also exchange their counterions for different counterions in the microsphere suspension, with typically significant consequences. Ion exchange is a slow process that required ∼2 weeks to equilibrate a small (∼600 μm diameter) anion exchange gel bead immersed in a pH 8.0 microsphere suspension.

Another potential problem with ionic (charged) gels is that the osmotic pressure of any polyelectrolyte solution, including a charged gel, relative to that of its bathing solution can be far greater than is the case for a corresponding neutral polymer or gel, and it varies strongly with the concentration of both the intrinsic charge and free electrolyte inside the gel. The large internal osmotic pressure strongly favors swelling, which is opposed by elastic deformation of the gel. Changes in electrolyte concentration inside the gel occur as a result of changes in the electrolyte concentration of the bathing solution. For example, a large decrease in electrolyte concentration of the external bath will induce a corresponding (but generally smaller) decrease in electrolyte concentration in the ionic gel, which may cause a substantial increase in its osmotic pressure. In an effort to reduce its concentration of intrinsic charges, the gel swells by directly absorbing liquid from the bathing solution, which in turn may generate some convective flow in the solution, and also raises the elastic free energy of the gel network.

In view of the complexities of charged gels, we are not able to quantitatively predict the temporal behavior of any free electrolyte concentration as it is released from, or absorbed into, the gel. For simplicity, we assume here that the gels are completely rigid and invariant in size, and simply provide a qualitative description of the ion transfers that occur, when a particular rigid gel that has been prebathed in one solution equilibrates with an infinite volume of another solution. The direction of the ion transfers determines the direction (inward vs outward) of ion-concentration gradients in the solution near the gel. The direction of the chemotactic forces and velocities follow from such gradients via eqs 1−9.

Results reported by the Pollack lab are summarized in Table 1. Of particular interest are those cases where either no exclusion or attraction instead of exclusion was observed. Our objective in this section is to understand in a qualitative way the various observations in terms of base/acid and salt gradients that are formed when the gel is placed in contact with an infinite solution of the same composition as the microsphere suspension (apart from the microspheres and their complement of counterions). Because the free acid or free base concentration inside the gel was generally not specified, we estimate it by calculations based on plausible assumptions regarding the contents of a prebath. In several cases, where no observation was reported, denoted by NR, we make predictions according to the present theory. Such predictions can be tested by further experiments.

Our basic plan is to calculate the concentrations of all ionic species inside the gel, taking into account any ionization equilibria of both mobile and fixed ions, when the gel is equilibrated with its specific prebath prior to being placed in contact with the microsphere suspension. In some cases, that prebath was pH 5.7 deionized water. The departure from pH 7.0 is attributed entirely to the presence of CO_2, HCO_3^-, and H^+ ions, and the concentrations of such species are reckoned simply from the pH and equilibrium constants for hydration of CO_2 and dissociation of carbonic acid. We then (1) apply Donnan conditions for all possible pairs of positive (p) and negative (n) mobile monovalent ions, $c_p^g c_n^g = c_p^b c_n^b$, where the superscripts b and g denote bath and gel, respectively; (2) adopt an assumed total concentration, c_0, and an appropriate dissociation constant for acid/base groups of the gel; and (3) impose an electroneutrality constraint on the gel, in order to obtain the concentrations of all ionic species, fixed and mobile, in the gel. In the case of a sulfonyl group, the H^+ dissociation constant ($K_d = 10^{+2.8}$, $pK_d = -2.8$) is so large that it is practically always ionized and its ionization equilibrium need not be considered. Likewise, quaternary ammonium groups are always ionized and there is no ionization equilibrium to consider. In some cases (e.g., Nafion 117 and ion exchange gels), the prebath composition is not independently known but is either inferred from other data or plausibly surmised. In any case, a second calculation is then carried out for each gel, when it is equilibrated with an infinite solution corresponding to that of the particular microsphere suspension (excluding the dilute microspheres and their complement of counterions). From changes in the concentrations of the various ionic species in the gel as it goes from its prebath to the microsphere suspension, the transfer of ions either into or out of the gel can be inferred. Because the calculations are rather tedious, we present complete calculations only for poly(acrylic acid) gel, which are provided in Appendix A. In this section, we merely summarize the results and conclusions of similar calculations for the various gels. Observations that likely involve convection are discussed at the end of this section.

I.1. Non-Ionic Gels. The first three gels in Table 1, namely, PVA, polyHEMA, and polyacrylamide, are non-ionic (neutral) and have no intrinsic charges. These gels are presumed to be thoroughly pre-equilibrated with deionized water at pH 5.7, and should behave exactly like PVA. As described in paper I (10.1021/jp302587d), PVA is expected to exclude carboxylated microspheres in suspensions of pH $\gtrsim$ 6.2 and amidinated microspheres in suspensions of pH $\lesssim$ 5.2. These predictions agree with the experimental results for all three gels. The not yet reported (NR) cases in Table 1 are predicted to exhibit normal exclusion. In addition, modest to negligible attraction is predicted for carboxylated microspheres in suspension of pH $\leq$ 5.2 and attraction is predicted for amidinated microspheres in suspensions with 6.2 $\leq$ pH $\leq$ 10.0. These latter predictions for non-ionic gels have not been tested.

These non-ionic gels of internal pH 5.7 are also predicted to exclude sulfated microspheres in suspensions with pH $\gtrsim$ 6.2, and to *attract* such microspheres in suspensions with 3.2 $\lesssim$ pH $\lesssim$ 5.2. These predictions, too, are so far untested.

I.2. Polyacrylic Acid Gel. A poly(acrylic acid) gel with c_0 = 0.01 M carboxyl groups is pre-equilibrated with a large volume of deionized water containing sufficient HCO_3^-, H_2CO_3, and CO_2(aq) to yield pH 5.7 (Appendix A). This gel is only weakly ionized ($f = 0.01$) because the H^+ concentration inside the gel is so high (10^{-4} M). When that same gel is equilibrated with a

solution containing the same total carbonate concentration ($c_{CO_2} + c_{H_2CO_3} + c_{HCO_3^-}$) plus sufficient NaOH to attain pH 8.0, it absorbs substantial NaOH, which contributes primarily to increase the ionized fraction from $f = 0.01$ to 0.29 (cf. Appendix A). Such NaOH uptake by the gel causes a deficit of NaOH in the solution near the gel surface, an outward gradient of $\ln c_{OH^-}$, and an outward force on any carboxylated microsphere in that region.

When the gel that was pre-equilibrated with pH 5.7 deionized water is then equilibrated with a solution obtained by adding sufficient HCl to the deionized water to achieve pH 4.0, it absorbs significant HCl from that solution. About 40% of the absorbed HCl is used to decrease the ionized fraction from $f = 0.01$ to 0.00704, and the remainder goes to increase the H^+ concentration inside the gel from 10^{-4} to 1.41×10^{-4} M (Appendix A). The uptake of HCl by the gel causes a deficit of HCl in the solution near the gel surface, an outward gradient of $\ln c_{H^+}$, and an outward force on amidinated microspheres.

These qualitative predictions agree with the observed exclusion of both carboxylated and aminated microspheres by poly(acrylic acid) gels under their respective experimental conditions.

I.3. Poly(acrylamide + malachite green) Gel. A gel consisting of a copolymer of acrylamide and a vinyl derivative of malachite green contains intrinsic positive charges on the malachite green moieties. Hence, its counterions must be negatively charged species, such as OH^-, HCO_3^-, or Cl^-. Malachite green is converted to a neutral, colorless carbinol by a hydrolysis reaction with a pK of 6.9. Thermodynamically, this reaction, $M^+ + H_2O \rightarrow MOH + H^+$, is indistinguishable from a proton dissociation reaction with pK = 6.9. When a gel with $c_0 = 0.01$ M malachite green groups is pre-equilibrated with a pH 5.7 prebath, the internal pH is 8.14, the concentration of positively charged malacite green groups (M^+) is $c_{M^+} = 5.48 \times 10^{-4}$ M, $c^g_{HCO_3^-} = 5.48 \times 10^{-4}$ M, and $c^g_{OH^-} = 1.37 \times 10^{-6}$ M. When the same gel is equilibrated with pH 5.7 deionized water plus sufficient NaOH to attain pH 8.0, the internal pH rises to 8.91, $c_{M^+} = 9.7 \times 10^{-5}$ M, $c_{HCO_3^-} = 8.97 \times 10^{-5}$ M, and $c_{OH^-} = 8.06 \times 10^{-6}$ M. By far, the largest concentration changes in the gel are the loss of 4.51×10^{-4} M c_{M^+} and 4.58×10^{-4} M HCO_3^- and gain of 6.7×10^{-6} OH^-. This change is accomplished by NaOH diffusing inward to the gel surface, exchange of the OH^- from the solution for an HCO_3^- from the gel, and diffusion of $NaHCO_3^-$ outward. In any quasi-steady state, the inward NaOH flux must nearly balance the outward $NaHCO_3$ flux. Because the diffusion coefficient of NaOH, $D_{NaOH} = 2.12 \times 10^{-5}$ cm^2/s, substantially exceeds that of $NaHCO_3$, $D_{NaHCO_3} = 1.25 \times 10^{-5}$ cm^2/s, the inward gradient of $NaHCO_3$ must exceed the outward gradient of NaOH by the ratio 2.12/1.25 = 1.7 in order to maintain a steady state. This in turn requires a net accumulation of Na^+ near the gel surface. Because $c_{salt} = c^b_{HCO_3^-} = 1.1 \times 10^{-5}$ M in the initial pH 8.0 solution exceeds $c^b_{OH^-} = 10^{-6}$ by more than 10-fold, the W term in F_{OH^-} is initially negligible compared to the 1.0 term (cf. eq 1). However, because $d \ln c_{salt}/dx = d \ln c_{HCO_3^-}/dx$ may become comparable to, or even exceed, the magnitude of $d \ln c_{OH^-}/dx$ in the quasi-steady-state (after accumulation of Na^+ near the gel surface) and is oppositely directed, F_{salt} may significantly cancel or even overcompensate F_{OH^-} in this case. The general prediction is that carboxylated microspheres should be either weakly excluded, neither excluded nor attracted, or weakly attracted by the malachite green gel. This range of predictions brackets the experimental observation of neither exclusion nor attraction.

I.4. Nafion Ionomer. The commercial Nafion 117 films employed by Pollack and co-workers are copolymers of tetrafluoroethylene and perfluoro vinyl ethers, some of which are terminated by $-SO_3H$ groups. These are not dilute gels but instead are ionomers that exhibit both semicrystalline hydrophobic regions and hydrophilic regions or channels containing clusters of modestly hydrated $-SO_3^-$ ions and their H^+ counterions. The dissociation constant for $-SO_3H$ is so low (p$K = -2.8$) that it is ionized even at very low hydration levels. Nafion emerges from the synthesis as the sodium salt, which is then converted to its protonic form by equilibration with a strong acid (pH $\lesssim$ 0), and then processed to produce the commercial film. Prior to some experiments, the Nafion was washed or soaked only briefly ($\leq$10 min) in deionized water, which is apparently insufficient for equilibration.[7] For these experiments, the effective prebath was the strong acid used by the maufacturer, which is here presumed to be HCl. Prior to other experiments, the Nafion film was equilibrated for a week with deionized water (pH 5.7), which can then be regarded as the prebath.[3]

When the prebath is the strong acid, the Nafion film contains some free acid that can be discharged into a surrounding solution of any pH greater than that (pH $\lesssim$ 0) of the prebath.[7] When it is immersed in a solution containing the same total carbonate concentration as pH 5.7 deionized water plus sufficient NaOH to attain pH 8.0 (cf. Appendix A), typical of the microsphere suspensions, significant free acid is released into the solution, and also H^+ counterions of the Nafion are exchanged for Na^+ ions of the microsphere suspension. These processes lead to an increase in c_{Cl^-} and decreases in c_{Na^+}, c_{OH^-}, and $c_{HCO_3^-}$ in the solution near the Nafion surface. Neutralization reactions cause the total electrolyte concentration ($c_S = c_{OH} + c_{salt}$) of the solution to fall. Two ions are lost in the reaction, $H^+ + OH^- \rightarrow H_2O$, so every Na^+ exchanged for an H^+ in this alkaline solution results in the loss of two ions to the solution. Similarly, the addition of an HCl to the solution, which provides an initial gain of two ions, is followed by the same neutralization reaction to lose two ions, so there is no net gain in electrolyte concentration of the solution upon transferring HCl from the gel to the solution. At pH 8.0, c_{OH^-} is somewhat buffered by HCO_3^- ions, which are initially present at ~11-fold higher concentration and undergo the hydrolysis reaction, $HCO_3^- + H_2O \rightarrow H_2CO_3 + OH^-$, to partially resupply the OH^- lost by neutralization. Nevertheless, there remains the net loss of a negative ion for every proton that undergoes a neutralization reaction in the solution. The end result is that near the Nafion surface: (1) c_{OH^-} is decreased, which yields an outward gradient of $\ln c_{OH^-}$ and an outward F_{OH^-}, and (2) c_S is decreased, giving an outward gradient of $\ln c_S$ and an outward electrolyte force F_S, which is the sum of F_{salt} (eq 2) and the second term in F_{OH^-} (eq 1). Hence, the total predicted force on carboxylated or sulfated microspheres is outward, in agreement with the reported exclusion in this case of an acid prebath.

When a Nafion film with the same acid prebath is immersed in a pH 2.5–4.0 HCl solution, typical of an amidinated microsphere suspension, the transfer of some free acid from the Nafion film to the solution still occurs, but in the absence of Na^+, the H^+/Na^+ exchange cannot occur. At the acidic pH of

the microsphere suspension, neutralization also does not occur, so c_S increases upon addition of HCl. In this case, the gradients of ln c_{H^+} and force, F_{H^+}, on the amidinated spheres are directed inward, and in the absence of salt, F_{salt} = 0. Thus, the amidinated microspheres are predicted to move *toward* the Nafion film in this case (i.e., *attraction* should be observed). Unfortunately, no results pertaining to this case were reported, so this remains an untested prediction.

When a Nafion film with a prebath of pH 5.7 deionized water is immersed in the standard pH 8.0 suspension containing sulfated microspheres, the transfer of free acid from film to solution is only very slight, but H^+/Na^+ exchange still occurs, leading to decreased c_{Na^+}, c_{OH^-}, $c_{HCO_3^-}$, and c_S, as before. This yields outward gradients of ln c_{OH^-} and ln c_S, hence an outward total force, and predicts exclusion of sulfated microspheres, as observed.

When a Nafion film with the same pH 5.7 prebath is immersed in a pH 2.5−4.0 HCl solution, typical of amidinated spheres, free acid is now transferred from the solution to the film, resulting in decreased c_{H^+} near the Nafion surface. In the absence of Na^+ ions, H^+/Na^+ exchange does not occur and c_{salt} = 0, so F_{salt} = 0. The decreased c_{H^+} near the Nafion surface yields an outward gradient of ln c_{H^+} and an outward force F_{H^+}. The total force ($F_{ch} = F_{H^+} + F_{salt}$) on the amidinated spheres is outward, in agreement with the observed exclusion.[3]

For the amidinated microspheres, the predicted direction of the force and motion depends entirely on the direction of free acid transfer, which in turn depends entirely on the difference between the pH of the prebath ($\lesssim$0 for the acid bath or ∼5.7 for the deionized water bath) and that (2.5−4.0) of the microsphere suspension. When the prebath is more acidic than the microsphere suspension, the predicted force is inward, and when it is more basic than the microsphere suspension, the predicted force is outward.

I.5. Agarose Gel. Agarose has a weak negative charge that arises primarily from sulfate ($-OSO_3^-$) groups, whose pK is so low that they remain fully ionized at all pH values ($\gtrsim$3.0) encountered in the experiments under discussion. The dilute agarose gel was pre-equilibrated with pH 5.7 deionized water. When such a gel is then immersed in a solution with the same total carbonate plus sufficient NaOH to attain pH 8.0, the main process that occurs can be regarded as the transfer of NaOH from the solution to the gel, and the annihilation of an equivalent number of H^+ counterions therein by reaction with OH^-. This has the effect of depleting c_{NaOH} in the solution near the surface of the gel. Also, in much smaller amounts, $NaHCO_3$ salt is transferred from the solution into the gel. These changes produce outward gradients of both ln c_{OH^-} and ln c_{salt} and outward forces, F_{OH^-} and F_{salt}, so exclusion of carboxylated microspheres from the agarose gel is predicted. Results for carboxylated microspheres were not reported, so this prediction remains untested.

When the same pre-equilibrated gel is immersed in a solution of pH 4.0 HCl which is sufficiently acidic to suppress adventitious HCO_3^-, it absorbs significant HCl from the solution. This produces on outward gradient of ln c_{H^+} and an outward F_{H^+} acting on amidinated spheres. This prediction agrees with the reported exclusion of amidinated microspheres.

I.6. Cation Exchange Gel. A cation exchange gel (a gel bead in the Bio-RexMSZ501(D) mixed-bed ion exchange resin) consists of cross-linked polystyrene divinyl benzene backbones functionalized with sulfonic acid ($-SO_3H$) groups. As noted in section I.4 above, the pK of $-SO_3H$ is so low that these groups are practically 100% ionized under all conditions considered here. The counterions of such a gel are H^+ ions, which were presumably obtained by equilibrating the $P-SO_3^-\cdot Na^+$ emerging from the synthesis with a concentrated strong acid (pH $\leq$ 0) prebath. In addition to exchanging the complement of Na^+ counterions for H^+ counterions, this process also deposits some free strong acid in the gel. The amount of the latter depends upon the concentration, c_0, of sulfonyl groups in the gel, and that of acid in the prebath. Significant free strong acid remains in the gel even after brief rinsing in pH 5.7 deionized water. This gel is expected to behave qualitatively like the Nafion film with the acid prebath but unlike the Nafion film with the distilled water prebath.

When this cation exchange gel is immersed in a solution containing the same total carbonate as pH 5.7 deionized water plus sufficient NaOH to attain pH 8.0 (cf. Appendix A), typical of carboxylated and sulfated microsphere suspensions, the ensuing changes are all qualitatively identical to those found for the Nafion film with the acid prebath in section I.4 above. Hence, the prediction is qualitatively the same, namely, an outward total force and exclusion of sulfated or carboxylated microspheres from the surface of the (negatively charged) cation exchange gel. This prediction agrees well with the reported exclusion of both carboxylated and sulfated microspheres.[4]

When this cation-exhange gel is immersed in a pH 2.5−4.0 solution, typical of an amidinated microsphere suspension, the changes are again all qualitatively identical to those found for the Nafion film *with the acid prebath*. Hence, the predictions are qualitatively the same, namely, an inward total force and consequent *attraction* of amidinated microspheres to the gel surface. This agrees very well with the reported inward migration of the amidinated microspheres to form successive dense layers or shells around the (negatively charged) cation exchange gel.[4] The density in each shell is so great that the microspheres therein exhibit apparent "crystalline" order. It should be carefully noted that this prediction changes to exclusion if the cation exchange gel (or the Nafion film) is first equilibrated with pH 5.7 deionized water, as discussed in section I.4 above.

I.7. Anion Exchange Gel. An anion exchange gel (a different kind of gel bead in the Bio-Rex MSZ501(D) mixed-bed ion exchange resin) consists of cross-linked polystyrene divinyl benzene backbones functionalized with quaternary ammonium ($-N^+(CH_3)_3$) groups. The positive charge on the nitrogen cannot be removed by titration, so these groups are 100% ionized under all conditions. The counterions of such a gel are OH^- ions, which were presumably obtained by equilibrating the $-N^+(CH_3)_3\cdot Cl^-$ emerging from the synthesis with concentrated strong base prebath (pH $\geq$ 14). In addition to exchanging the complement of Cl^- counterions for OH^- counterions, this process also deposits some free strong base in the gel. The amount of the latter depends upon the concentration, c_0, of quaternary ammonium groups in the gel and that of base in the prebath. Significant free strong base remains in the gel even after brief rinsing in pH 5.7 deionized water.

When such a gel is equilibrated with an infinite solution of pH 2.5−4.0 HCl, typical of an amidinated microsphere suspension, OH^- counterions in the gel are exchanged for Cl^- ions of the solution and some of the free NaOH is transferred to the solution. These processes lead to an increase

dx.doi.org/10.1021/jp302589y | J. Phys. Chem. B 2013, 117, 7653−7674

in Na^+ and decreases in c_{Cl^-} and c_{H^+} in the solution near the gel surface. Neutralization reactions cause the total electrolyte concentration ($c_S = c_{H^+} + c_{salt}$, in this case) of the solution to fall. Each Cl^- exchanged for an OH^- from the gel results in a loss of two ions by the reaction $OH^- + H^+ \rightarrow H_2O$. Addition of free NaOH initially increases the number of ions by two, but the OH^- undergoes a subsequent neutralization reaction to eliminate two ions, so there is no net gain in electrolyte concentration upon adding NaOH. The end result is that near the Nafion surface: (1) c_{H^+} is decreased, which yields an outward gradient of $\ln c_{H^+}$ and an outward F_{H^+}, and (2) c_S is decreased, giving an outward gradient of $\ln c_S$ and an outward electrolyte force, F_S, which is the sum of F_{salt} and the second term in F_{H^+} (eq 3). Hence, the total predicted force on the amidinated spheres is outward, in agreement with the reported exclusion of amidinated microspheres.[4]

When this anion exchange gel is immersed in a solution containing the same total carbonate as pH 5.7 deionized water plus sufficient NaOH to attain pH 8.0 (cf. Appendix A), typical of carboxylated and sulfated microsphere suspensions, OH^- from the gel is exchanged for HCO_3^- from the solution, and some NaOH is released from the gel to the solution. By these processes, c_{Na^+} and c_{OH^-} are increased and $c_{HCO_3^-}$ is decreased near the gel surface. In alkaline solutions, such changes result in no significant neutralization reactions, so the net electrolyte concentration, $c_S = c_{Na^+} + c_{OH^-} + c_{HCO_3^-}$, is increased (by the transfer of NaOH to the solution) near the gel surface. As a consequence of these changes, (1) the gradients of $\ln c_{OH^-}$ and F_{OH^-} are directed inward and (2) the gradients of $\ln c_S$ and F_S are directed inward. Hence, the predicted total force on sulfated or carboxylated microspheres is directed inward. This agrees well with the reported inward migration of sulfated microspheres from distances of several hundred μm to form successive dense layers or shells extending $\geq$16 μm (equivalent to $\geq$48 Debye lengths) outward from the (positively charged) anion exchange gel.[4] The density in each shell is so great that the microspheres therein exhibit apparent "crystalline" order.

The regularity of the sulfated microspheres in the "crystalline" dense layers around an anion exchange gel appears to be even greater than that exhibited by amidinated spheres around a cation exchange gel,[4] and likely reflects a greater microsphere density. This suggests that the total inward force is greater for the anion exchange gel than for the cation exchange gel. Possible reasons for this are as follows: (1) the amount of free base released from the anion exchange gel to the pH $\gtrsim$ 8.0 suspension of the sulfated microspheres may significantly exceed the amount of free acid released from the cation exchange gel to the pH 2.5−4.0 amidinated sphere suspension; (2) the number of surface groups of the sulfated microspheres exceeds that of the amidinated microspheres, which is commonly the case; (3) collective interactions between microspheres may be less repulsive or more attractive for the sulfated than for the amidinated species. It is conceivable that one, two, or all three of these possible reasons contribute to the greater density of the sulfated microspheres around anion exchange gel beads.

I.8. Microsphere Bridge Crystals. Symmetric multilayer bridge crystals of dense sulfated microspheres were observed to form between two large (600 ± 100 μm diameter) anion exchange gel beads, when they were sufficiently close together (surface-to-surface gap $\lesssim$50−55 μm).[4] These bridges were widest near the gel surfaces and narrowest at the midpoint between the two beads. We suggest that this phenomenon arises primarily from the gradients of $\ln c_{OH^-}$ and their associated forces that result from overlap of the "plumes" of strong base diffusing outward from each gel bead. An effective multisphere mutual attraction among moderately dense microspheres may also contribute to the formation of the dense crystalline array, especially near the center of the bridge crystal, where the gradient of $\ln c_{OH^-}$ and its associated force must vanish. Bridge crystals between two anion exchange gel beads could be observed only for the attracted sulfated microspheres but not for the excluded (amidinated) microspheres.[4]

Interestingly, no bridge crystals of attracted amidinated microspheres could be found between two large (600 ± 100 μm diameter) cation exchange gel beads. This may be a consequence of a smaller inward force in this case, which may be attributable to any of the three reasons noted in section I.7 above. Not surprisingly, no bridge crystals between cation exchange gel beads were formed by excluded sulfated microspheres.[4]

Asymmetric multilayer bridge crystals of sulfated microspheres were also formed between an anion exchange gel bead and a cation exchange gel bead.[4] The width of the bridging "crystal" (in planes perpendicular to the interbead axis) tapered down continuously from the surface of the anion exchange gel bead to that of the cation exchange gel bead. We suggest that this phenomenon occurs because much more free base (presumably NaOH) is released by the anion exchange bead than free acid (presumably HCl) by the cation exchange bead. This yields a relative excess of c_{OH^-} in a zone of steadily diminishing width extending from the anion exchange gel surface toward the cation exchange gel surface. The associated gradient of the $\ln c_{OH^-}$ provides the dominant force that attracts the sulfated microspheres into that zone, whereupon a crystalline array is formed. A greater release of NaOH by the anion exchange bead than release of HCl by the cation exchange bead perhaps stems from either (1) a greater concentration of base in the prebath of the anion exchange bead than of acid in the prebath of the cation exchange bead or (2) more extensive rinsing/soaking of the latter with distilled/dionized water prior to the experiment.

When two anion exchange gel beads were initially very close together (edge-to-edge $\lesssim$5 μm) in the presence of a sulfated microsphere suspension, the beads "tended to come closer and touch one another", while the microspheres "nevertheless remained highly ordered in the intervening crevices near the contact point". We suggest that the system free energy declines when the gel beads move together and touch, because (1) the touching bead configuration may provide larger values and gradients of $\ln c_{OH^-}$ and larger forces F_{OH^-} over a much wider range in planes normal to interbead axis, so that more microspheres are actually incorporated into the bridge crystal at any given time, and (2) the electrolyte concentration experienced by the proximal surfaces of the anion exchange gel beads is greater the closer they are together, which diminishes their electrostatic self-energies.

I.9. Disappearance of Microsphere Crystals with Time. After approximately 2 weeks in the experimental chamber, the crystalline shells of sulfated microspheres around the anion exchange gel bead disappeared (i.e., the microspheres were dispersed).[4] Contemporaneously, the indicator dye incorporated into the gel changed color, indicating a decline of c_{OH^-} inside the gel, presumably due to exchange of OH^- inside the gel for HCO_3^- from the solution. After practically all of the

dx.doi.org/10.1021/jp302589y | J. Phys. Chem. B 2013, 117, 7653−7674

OH^- counterions inside the anion exchange gel have been exchanged for HCO_3^- (or any other adventitious anions in the microsphere suspension), the inward gradients of $\ln c_{OH^-}$ and $\ln c_{salt}$ around the gel should disappear, and their associated forces on the microspheres should vanish. In that event, sulfated microspheres should be neither attracted to nor excluded from the gel, as was observed.

I.10. Salt-Induced Disappearance of Microsphere Crystals. Addition of 0.01 M NaCl to the sulfated microsphere suspension suffices to disperse the crystalline shells of microspheres around the anion exchange gel bead.[4] We note that some of the added salt is incorporated into the gel (albeit at a significantly lower concentration than in the external solution) in order to establish (Donnan) equilibrium of the salt inside and outside the gel. This transfer of salt from solution into the gel depletes the concentration of added salt in the solution near the gel surface, which opposes (and possibly overwhelms) the increase of electrolyte due to NaOH transfer from the gel to the solution. This either diminishes or reverses the sign of the formerly inward electrolyte gradient. We suggest that this reduction or reversal of the inward electrolyte force diminishes the total inward force sufficiently that sulfated microspheres cannot be attracted sufficiently strongly to achieve a density necessary for "crystal" formation.

I.11. Microsphere Exclusion in Buffer. When suspended in 0.01 M pH 7.0 imidazole buffer, sulfated microspheres were excluded from both anion exchange and cation exchange gel beads, and the exclusion was greater in the case of the cation exchange gel.[12]

In the case of the negatively charged cation exchange gel, two main transfer processes contribute to concentration gradients in the surrounding solution. First, release of free acid (HCl) from the gel increases the local HCl concentration, most of which reacts with Im to produce the $ImH^+{\cdot}Cl^-$ salt. This process leads to a modest decrease in $c^b_{OH^-}$ and an increase of nearly two ions per released HCl in the total electrolyte (HCl + $ImH^+{\cdot}Cl^-$) near the anion exchange gel. The second, and dominant, process is the diffusion of neutral Im into the gel, whereupon it reacts with H^+, until practically all of the H^+ counterions are converted to ImH^+ counterions. This process continues until c^g_{Im} in the gel matches the c^b_{Im} in the bath. Due to protonation inside the gel, c^g_{Im} remains very small until the late stages of this process, which causes a large decrease in c^b_{Im} near the gel, which is locally largely relieved by the dissociation of ImH^+ to produce Im and H^+. This dissociation process raises the H^+ concentration significantly but does not affect the Cl^- concentration, or the total electrolyte concentration ($c^b_S = c^b_{HCl} + c^b_{ImH^+{\cdot}Cl^-}$) near the gel. The net result of the two combined processes is a significant relative increase in c^b_{HCl}, a corresponding relative decrease in $c^b_{OH^-}$, and a large outward gradient of $\ln c^b_{OH^-}$, as well as a modest increase in c^b_S near the gel. The latter provides only a small relative increase in c^b_S, which was initially 10 mM $ImH^+{\cdot}Cl^-$, so the gradient of $\ln c_S$ should be rather modest in magnitude and directed inward. Because $c^b_{OH^-} \ll c^b_{salt}$, the second (or W) term in F_{OH^-} is negligible, but the remaining first term (due to OH^- binding to $-OSO_3H$ groups) is outward and should dominate the electrolyte force, F_S. F_S has a small but significant contribution from HCl as well as from $ImH^+{\cdot}Cl^-$, and is directed inward. Thus, a moderate outward net force and moderate exclusion are expected, as was observed.

In the case of the positively charged anion exchange gel, three main transfer processes contribute to concentration gradients in the surrounding solution. First, release of free base (NaOH) from the gel increases the local NaOH concentration, most of which reacts with $ImH^+ + Cl^-$ to produce Im + NaCl. This process leads to an increase in both c^b_{NaOH} and c^b_{NaCl} and a decrease in $c_{Im^+Cl^-}$ near the gel bead, and an increase in total electrolyte by about two ions per released NaOH. The second (and dominant) process is the exchange of Cl^- from the solution for OH^- from the gel. This removes Cl^- and deposits a large amount of OH^- into the solution near the gel, which in turn converts considerable ImH^+ into Im, and thereby considerably diminishes the total electrolyte ($c_S = c_{NaCl} + c_{ImH^+{\cdot}Cl^-}$) near the gel (by about two ions per Cl^-/OH^-exchange). The third process is the diffusion of neutral Im into the gel until c^g_{Im} matches c^b_{Im}. The loss of Im from the solution is largely compensated by the dissociation of ImH^+ to $Im + H^+$, which in turn acts to neutralize a small part of the OH^- produced by the first two steps, and along with the loss of Cl^- in the second process acts to further reduce the concentration of $ImH^+{\cdot}Cl^-$ salt near the gel. This overall decrease in $c_{ImH^+{\cdot}Cl^-}$ should considerably exceed the increase in c^b_{NaOH}. The net result of the combined three steps is most likely a moderate relative increase in c^b_{NaOH}, which yields a moderate inward gradient of $\ln c^b_{OH^-}$, and a significant relative decrease in total salt concentration ($c^b_{salt} = c^b_{NaCl} + c^b_{ImH^+{\cdot}Cl^-}$), which yields a significant outward gradient of $\ln c^b_{salt}$. As before, the second term in F_{OH^-} is negligible. Because a firm estimate of W is not available, we cannot estimate reliably the ratio, $|F_{salt}/F_{OH^-}|$, of the outward F_{salt} to the inward F_{OH^-}. If $|F_{salt}/F_{OH^-}|$ exceeds 1.0, which is not unlikely, then exclusion would be predicted. A firmer prediction will require a precise value of W and accurate modeling of the ion transfers between the gel and the solution.

In this section, we have proposed plausible qualitative explanations for several interesting phenomena that are exhibited subsequent to immersion of charged gels in suspensions of carboxylated, sulfated, or amidinated microspheres. All explanations are based on the present theory of chemotactic forces arising from gradients of $\ln c_{OH^-}$, $\ln c_{H^+}$, $\ln c_{salt}$, or $\ln c_S$, where S denotes total electrolyte. The qualitatively diverse experimental observations of Pollack and co-workers provide non-trivial tests of this theory of macromolecular chemotaxis. The rather good agreement between predictions of the theory and the reported observations suggests that all of these exclusion and attraction phenomena might be attributable primarily to chemotaxis of the microspheres in non-equilibrium base/acid gradients and salt or total electrolyte gradients.

I.12. Exclusion of Much Smaller Species. Zheng et al. observed that a fluorescence-free zone was formed around a Nafion 117 film, when it was immersed in a solution of fluorescein-labeled BSA, or in a solution containing simply fluorescein.[2] This zone widened to ~100 μm by 1000 s after immersion. It was concluded that BSA and fluorescein were excluded from the fluorescence-free region. Chemotaxis theory is applicable to BSA (as demonstrated in paper I, 10.1021/jp302587d) and in principle applies also to fluorescein. The fluorescence experiments would be quantitatively consistent with predictions of the chemotaxis theory, if the ratios, λ/A_1, for microspheres, BSA, and fluorescein did not differ too greatly. Although this interpretation remains a possibility, an alternative interpretation of the experiments also merits consideration.

The fluorescence intensity of fluorescein falls off rapidly below pH 7.0, and is undetectable below pH 3.[18] The release of excess free acid from the Nafion 117 film evidently drives the pH of the neighboring unbuffered bath far below pH 7.0.[7]

Thus, the fluorescence from both the fluorescein-labeled BSA and from the free fluorescein should be quenched by the outward-diffusing plume of free acid. Because little or no fluorescence is expected from any such molecules within that part of the plume where pH $\lesssim$ 6.0, the exclusion of such molecules cannot be directly inferred from the absence of their fluorescence.

An apparent exclusion zone was also observed, when a Nafion film was immersed in a solution containing the fluorescent zwitterionic dye, 6-methoxy-*N*-(3-sulfopropyl)-quinolinium.[3] However, it is well-known that the fluorescence of this dye is quenched by Cl^- ions, which may be transferred as part of the free acid from the Nafion to the solution, so the apparent exclusion could be simply a quenching effect due to an enhanced Cl^- concentration near the Nafion surface. In addition, the reported fluorescence image indicates that this dye is strongly absorbed by the Nafion into regions where it is not strongly quenched.[3] Such absorption would reduce the prevailing dye concentration in the solution near the gel surface, which could be mistaken for exclusion.

In order to demonstrate conclusively the exclusion of dyes, or dye-labeled proteins, one must use dyes that are neither quenched by ions transferred from Nafion to the solution nor strongly absorbed by the Nafion.

I.13. Exclusion Zones in Other Polar Solvents. Chai and Pollack reported that carboxylated and sulfated microspheres of 1 μm diameter suspended in any of several polar solvents (H_2O, D_2O, methanol, ethanol, acetic acid, isopropanol, and dimethylsulfoxide (DMSO)) developed exclusion zones of width 31−220 μm, depending upon the solvent, near the surface of a section of Nafion tubing. In addition, amine coated microspheres in ethanol and isopropanol also developed exclusion zones around the same tubing. The Nafion was immersed in each particular solvent for 10 min prior to immersion in a microsphere suspension in that same solvent. The Nafion swelled substantially more in non-aqueous polar solvents than in water,[7] which raises the possibility that free acid transfer from the Nafion to the non-aqueous solvent in 10 min might be much better equilibrated than is the case in water. The microsphere suspensions were prepared by first drying the corresponding aqueous suspension and then suspending the residue, including any excess base or acid, in the particular non-aqueous solvent. The carboxylate and sulfate microspheres typically come with excess base (e.g., NaOH). Consequently, the extent of equilibration of the Nafion with the pure solvent prebath does not affect the qualitative predictions of subsequent net transfer of free acid from the Nafion to the basic suspension and outward gradients of $\ln c_{OH^-}$ and $\ln c_{salt}$ (salt = $NaHCO_3$), hence outward forces on carboxylate or sulfate spheres, in agreement with the experimental observations. However, the extent of equilibration of the free acid transfer from Nafion to a given non-aqueous solvent does affect the predicted direction of the H^+ gradient and force on the amino microspheres, which typically come with excess acid. If the free acid transfer between the Nafion and a large reservoir of pure solvent is nearly equilibrated, then when that Nafion is placed in contact with a significantly acidic microsphere suspension, free acid will transfer from the suspension to the Nafion, thereby creating an outward gradient of $\ln c_{H^+}$ and an outward force (F_{H^+}) on amino microspheres. However, if sufficient free acid remains in the Nafion after 10 min in a large reservoir of pure solvent, as is apparently the case in water,[7] then transfer of free acid from the Nafion to a microsphere suspension with $10^{-2.5}$−10^{-4} M excess acid may occur, which would result in an inward gradient of $\ln c_{H^+}$ and an inward force (F_{H^+}) on amine coated microspheres. In the absence of any certain information regarding the direction of free acid transfer between a Nafion film, which was prebathed for 10 min in pure solvent, and an acidic suspension of microspheres in that same solvent, it is not possible to make a reliable prediction regarding the direction of the force on amino microspheres in ethanol or isopropanol.

I.14. Observations That May Involve Convection. Several observations of Pollack and co-workers that likely involve convection are addressed in this section. Convection may result from a variety of mechanisms, including the following.

(a) Any solution with a gradient of c_{OH^-} or c_{salt} in contact with a glass surface (or other negatively charged surface bearing OH^--binding groups) experiences a force so as to move the solution toward the less basic and/or less salty end of the gradient, as discussed toward the end of the Introduction.

(b) A gradient of surface tension (γ) at the air−solution interface, such as that associated with a gradient of either surfactant concentration or surface temperature, induces convection of the surface and its underlying solution.[19] The quantity $\partial\gamma/\partial x$ constitutes a tangential force per unit area acting in the x-direction on a given element of the air−solution interface. This force must be opposed by a viscous traction, $-\eta\partial v_x/\partial z$ (where z lies along the upward surface normal) that is exerted by the underlying solution on the same surface element, so that its total force per unit area vanishes. Hence, $\eta\partial v_x/\partial z = \partial\gamma/\partial x$ at the air−solution interface and the shear gradient ($\partial v_x/\partial z$) near the top surface has the sign of $\partial\gamma/\partial x$, from which movement of the top layer in the $\partial\gamma/\partial x$ direction can be inferred. In fact, such motion (Marangoni convection) can also generate a complete convection cell.[19]

(c) A decrease in total volume (e.g., due to electrostriction) upon swelling a gel or ionomer causes net inward fluid flow.

(d) Motion of the center of drag of a gel or ionomer normal to the chamber surface upon which it resides necessarily accompanies any change in its extent of swelling, and displaces external solution.

(e) Asymmetry of any change in extent of swelling also displaces solution external to the gel.

(f) Osmotically induced flow across a gel or ionomer membrane necessarily involves a convection component normal to the membrane surface.

Pertinent observations of Pollack and co-workers are noted below, and in each case, one or more possible mechanisms by which convection might be involved are suggested and briefly discussed.

A non-monotonic increase of exclusion zone size with increasing time was observed for Nafion in ethanol, wherein Nafion swells asymmetrically and significantly more than in water.[9] In principle, any or all of mechanisms a−e could induce convection and perhaps initiate a convection cell to provide cyclic motion of the fluid. That in turn could lead to non-monotonic variation of the chemotactic forces and microsphere positions with increasing time. The difference in behavior between ethanol and water, where exclusion zone growth is monotonic, may arise from a difference in their ability to swell Nafion, and/or in other properties including surface tension, slip length, viscosity, dielectric constant, and density, all of which may affect convection.

The size of the exclusion zone formed by negatively charged microspheres (carboxylate, sulfate, or silicate) near a Nafion

surface was found to increase upon irradiation with infrared (IR) light of wavelength 3.1 μm, which is resonant with the −OH stretching vibration of water.[7] Such light has an absorption length of L = 1.26 μm in water.[20] L is the distance over which the intensity of incident radiation falls to exp[−1] times its initial value. In this case, 98% of the incident radiation is absorbed within 5 μm of the surface, and the rise in surface temperature of the illuminated region should exceed by many-fold the reported increase (∼1.0 °C) of the bulk average temperature.[7] The surface temperature gradient near the boundary of the illuminated region might then suffice to induce convection via a Marangoni effect (mechanism b). Convection near, but outside, the gel generally acts to stir the solution, sharpen the gradient near the Nafion surface, and increase the net rate of outward transport of acid from the Nafion surface, which in turn should extend the average gradients of $\ln c_{OH^-}$ and $\ln c_S$ and increase the apparent exclusion zone size, as observed.

During osmotically induced water flow through a semi-permeable gel or ionomer (Nafion) membrane, some parts of the surface on the water side of the membrane did not exhibit exclusion zones, whereas other parts of the same surface did.[21] However, the ∼50−120 μm widths of those (Nafion) exclusion zones are somewhat smaller than the usual values (∼200−220 μm) for Nafion at 5 min after immersion in a suspension of sulfate microspheres. According to mechanism f, inward flow of water toward the membrane on its water side would be expected, and that should oppose the outward diffusion of excess acid and exchanged protons, thereby partially or entirely compressing the exclusion zone. If the permeability or porosity of the membrane is non-uniform over its surface, then the normal component of convective flow will vary from one part of the surface to another, and the degree of compression of the exclusion zones will vary accordingly. Regions of highest permeability/porosity may have almost completely compressed (apparently non-existent) exclusion zones, whereas those that sufficiently impede transmembrane flow may have exclusion zones of more normal size. This would match the observations. Unfortunately, independent information concerning variations in permeability/porosity over the membrane surface is not available. However, if the present interpretation is correct, then variation of exclusion zone width over the surface might eventually provide a way to assess the variation in permeability. Zhao et al.[22] reported slow (∼0.3 μm/s) inward translation of sulfate microspheres from a distance of ∼2 mm to ∼300 μm from the outer edge of either an attraction zone around a (positively charged) anion exchange gel bead or an exclusion zone around a (negatively charged) cation exchange gel bead. This surprisingly uniform inward translation over such a large distance is almost surely a manifestation of slow inward convection, which is overwhelmed by microsphere chemotaxis at distances ≲300 μm from the surfaces of the ∼600 μm diameter gel beads. Mechanism a is eschewed, because the OH^- and electrolyte gradients surrounding the positively and negatively charged beads are in opposite directions, yet this outer flow is inward for both. Quantitative estimates suggest that, for any plausible swelling rate, mechanism d is insufficient. The absence of visible asymmetry of swelling argues against mechanism e. If the observed relative rate of volume loss during osmotic flow[21] applies generally to Nafion films immersed in microsphere suspensions, then calculations indicate that mechanism e is grossly insufficient to account for the observed inward volume flux of fluid. However, mechanism b could be involved in the following way. If surface-active compounds diffuse out of the ion exchange gel bead or out of the Nafion film, they will preferentially adsorb to the air−solution interface above their place of origin, decrease the local surface tension, and thereby create an outward gradient of surface tension, which in turn leads to an outward radial Marangoni flow of the top layer of the solution. The surface-active species could be low molecular weight prematurely terminated ionic or non-ionic polymers, polymerization initiators, or plasticizers. The outward Marangoni flow could lead to fluid pile-up near the outer chamber boundaries, build-up of a pressure gradient, and eventually formation of a complete convection cell. It has been demonstrated that continuous addition of a surface-active compound to a central location on top of a 0.07 m deep and 0.13 m wide water layer leads quickly to a steady convection cell with a rapid (∼0.5 m/s), cylindrically symmetric, outward, radial Marangoni flow in a very thin (5×10^{-4} m) top layer and a ∼100-fold slower inward radial flow in the lower layers.[19] The inverted microscope(s) used by Zhao et al.[22] limit their observations to particle motions primarily in the lower layers. Large quantitative, and possibly even qualitative, changes in behavior might result from reducing the fluid depth and width to the dimensions in the experiments of Zhao et al.[22] Nevertheless, the possibility that slow inward microsphere motion beyond an attraction or exclusion zone is due to slow inward radial flow of the bottom layer of a Marangoni convection cell merits serious consideration. Because the inward flow velocity of such a cell declines from its maximum toward zero with decreasing height above the floor of the chamber, there should be a region near the outer boundary of the exclusion zone, where microspheres closer to the bottom move outward (outward chemotaxis relative to fluid exceeds inward fluid velocity relative to stationary bottom), whereas microspheres farther from the bottom move inward (inward fluid velocity relative to stationary bottom exceeds chemotaxis relative to fluid), as was reported. A search for a thin upper layer with a rapid outward radial velocity might confirm the existence of a Marangoni convection cell in such experiments.

The effects of convection induced by gradients of $\ln c_{OH^-}$ and $\ln c_S$ in contact with the bottom glass surface are not apparent in the experiments of Zhao et al.,[22] presumably because the ratio of microsphere velocity to fluid velocity *induced by this mechanism* always substantially exceeds 1.0. This circumstance is attributable in large part to the rather small fraction f of ionized silanol groups (cf. Appendix E of paper I, 10.1021/jp302587d).

Convection is plainly apparent in those experiments, demonstrating the movement of two anion exchange gel beads toward one another.[6] The anion exchange gel beads release excess NaOH (or other hydroxide) to the solution, and for two close-lying beads, the NaOH concentration is significantly higher between the two beads, especially at their proximal (front side) surfaces, than at their distal (back side) surfaces. These beads with quaternary ammonium charges do not participate in an H^+ dissociation/binding equilibrium, so their direct interaction with the solution, apart from release of NaOH or exchange of OH^- for HCO_3^- from the solution, is simply the lowering of their electrostatic free energy by the released electrolyte (NaOH), which is present at highest concentration between the two beads. Thus, the overall system free energy should decline as the two beads move closer together into the region of highest electrolyte concentration. This might be the main driving force for the observed motion.

dx.doi.org/10.1021/jp302589y | J. Phys. Chem. B 2013, 117, 7653−7674

Mechanisms a–e above might be involved in the observed convection of the NaOH plumes,[6] but the origin of the plume asymmetry remains obscure. Whether convection makes a significant or perhaps even dominant contribution to the bead motion is not known.

The cation exchange gel beads release excess HCl to the solution, and for two close-lying beads, the HCl concentration is higher between the two beads, especially at their proximal surfaces, than at their distal surfaces. In this case, the OH^--binding force is negligible compared to the electrolyte force for the following reason. These gel beads bear sulfonate groups, which in principle were formed by the OH^--binding reaction, $-SO_3H + OH^- \rightleftharpoons -SO_3^- + H_2O$, which has an intrinsic equilibrium constant, $K_b = K_a^d/K_w = 10^{16.8}$, where $K_a^d = 10^{2.8}$ is the intrinsic equilibrium constant for the acid dissociation reaction, $-SO_3H \rightleftharpoons -SO_3^- + H^+$, and $K_w = 10^{-14}$ is the self-ionization constant of water. Electrostatic interactions between groups on the microsphere are assumed to shift the apparent pK_a^d by +1.50 at the midpoint of the (theoretical) titration curve, which yields an apparent OH^- binding constant, $K_b = 10^{15.3}$, at that point. The forward rate constant of the diffusion-controlled bimolecular OH^- binding step is $\vec{k} \cong 10^{10}\ M^{-1}\ s^{-1}$, and the reverse rate constant for the OH^- dissociation step is $\overleftarrow{k} = \vec{k}/K_b \cong 10^{-5.3} = 2.01 \times 10^{-6}\ s^{-1}$. Hence, the mean dissociation time is $\tau_{diss} = 1/\overleftarrow{k} = 2.0 \times 10^5$ s. The requilibration time is $\tau = \tau_{diss} + \tau_{bind}$, where $\tau_{bind} = 1/(\vec{k}\, c_{OH^-})$. For $c_{OH^-} = 10^{-3}$ M, one has $\tau_{bind} = 10^{-7}$ s and $\tau \cong 2.0 \times 10^5$ s. For a velocity $u = 0.0004$ cm/s, the equilibration condition, $\tau u \partial \ln c_{OH^-}/\partial x \leq 0.1$, requires $\partial \ln c_{OH}/\partial x \leq 0.00125\ cm^{-1}$. Even for a much smaller $c_{OH^-} = 10^{-11}$ M, one has $\tau_{bind} = 10.0$, $\tau = 2.0 \times 10^5$, and $\partial \ln c_{OH^-}/\partial x \leq 0.00125\ cm^{-1}$. These upper limit gradients of $\ln c_{OH^-}$ are $\sim 10^{-5}$-fold smaller than those ($\sim 125\ cm^{-1}$) actually prevailing around the cation exchange gel beads at time $t = 20$ s in the experiments. Because the observed mean velocities of $\sim(3.3–5.0) \times 10^{-4}$ cm/s (with 2–3 taps per second) over the first 50–75 s are close to the assumed $u = 4.0 \times 10^{-4}$ cm/s, we conclude that equilibration of the sulfonic acid binding reaction is far too slow to keep up with the observed bead motion in the experimental gradients. In such a circumstance, the actual OH^--binding force on the bead is far less than that reckoned via the first term in eq 1, so the electrolyte force, F_S, is expected to predominate, as was the case for the quaternary ammonium groups of the anion exchange gel beads. Again, the system free energy is lowered by bead motion toward higher electrolyte concentration, which lies between the two spheres. As before, this might be the main driving force for the observed motion of the beads toward one another. However, the possibility that convection might contribute to, or even dominate, the driving force cannot be ruled out, until its origins and flow patterns are better understood.

II. Long-Range Electrostatic Potentials. The electrostatic potential difference between a microelectrochemical electrode in the exclusion zone and a similar electrode in the region far beyond the exclusion zone was measured as a function of the distance of the former electrode from the gel or ionomer surface.[2,3,5,6,8,9] In the case of negatively charged gels and ionomers, the measured potential was −120 to −200 mV near the surface and declined with a steadily decreasing gradient to a negligibly small value at a distance ≥200 μm. For positively charged gels, the potential was similar in magnitude at all distances but positive. These potentials were measured with reversible Ag/AgCl(s) microelectrodes with internal 3.0 M KCl reservoirs that contacted the solution via very small capillary tubes. These voltage differences were ascribed to an accumulation of net negative charge in the ordered water of the exclusion zone,[2–4,7] which was also purported to be "largely free of mobile charge carriers" so as to prevent neutralization.[2] However, except very near the hydrophilic surface, the magnitude of the potential was strongly and differently affected by 1 mM concentrations of LiCl, NaCl, or KCl.[2,3] The potential was also found to be continuous across the gel/solution or Nafion/solution boundary.

The interpretation of the measured potentials in terms of ordered water with a net negative charge and immobile charge carriers is confronted by many problems, including the following.

The measured potentials involve reversible chemical reactions at the electrodes and do not arise simply from a particular distribution of fixed charges in the container, wherein the electrodes are positioned. Such an *electrochemical* potential is that supplied to the external circuit by an adjustable external electromotive force ($\mathcal{E}$) so as to precisely cancel the current arising from a divided (into half-cells) redox reaction, whose electron transfer takes place via the same external circuit. If the number of electrons (n) transferred per net reaction (sum of the half-reactions taking place in the cathode and anode half-cells) is known, then $\Delta G = -nF\mathcal{E}$ is the reversible work or free energy change per mole of the redox reaction under the prevailing conditions at constant T and P. The factor $F = 96\,500$ C/mol of protonic charge is the Faraday. Thus, $\mathcal{E}$ (together with n) is a thermodynamic measurement rather than a direct electrostatic measurement of the kind that could be obtained using bare silver electrodes. This can be seen by a simple example.

Consider a concentration cell, where KCl is present in the cathode half-cell at one dilute concentration (c_1) and in the anode half-cell at another (c_2). When these two electroneutral solutions are connected by a KCl-containing salt bridge and the Ag°|AgCl(s)|3.0 M KCl electrodes are connected to opposite ends of the external circuit, the liquid junction potentials are negligibly small (because K^+ and Cl^- have very similar mobilities), and the measured electrochemical potential is given by $\mathcal{E} = -(RT/F)\ln(c_1/c_2)$, where $R = 8.316$ J/mol is the gas constant. Hence, a non-vanishing electrochemical potential is obtained for an electroneutral system with no fixed charges, and depends only upon the ratio of KCl concentrations in the two cells. There is clearly no reason to attribute such potentials to fixed charges in this system.

The contention that exclusion zones are largely free of mobile charge carriers[2] would imply that mobile ions could not penetrate into non-ionic hydrophilic gels, which should then exhibit ultralow conductivities. However, as already noted, soluble salts readily penetrate agar gels and their measured diffusivities (diffusion coefficients) in such gels are practically the same as in bulk solutions.[12] According to linear response theory, the conductivities of such species are proportional to their diffusion coefficients and concentrations, and consequently should be practically the same in the gel as in solution, as has been often observed for dilute non-ionic or weakly ionic gels. Indeed, thousands of gel electrophoresis experiments performed daily provide abundant evidence that mobile small ions (as well as proteins and nucleic acids) can penetrate into dilute agarose and polyacrylamide gels and readily conduct electric current through them.

dx.doi.org/10.1021/jp302589y | J. Phys. Chem. B 2013, 117, 7653–7674

If penetration of the exclusion zone by salt ions were not possible, then all univalent salts, such as LiCl, NaCl, and KCl would be expected to screen the exclusion zone potential in the same way due to their similar equilibrium concentration profiles external to the exclusion zone. However, LiCl, NaCl, and KCl were found to alter the measured potential near a Nafion film to very different extents,[2] which implies that they must have penetrated the exclusion zone, and possibly also the Nafion film.

Measurements with a pH-sensitive dye revealed a region of high proton concentration exterior to the exclusion zone of an anionic ionomer (Nafion), which was interpreted as net positive charge separated from the net negative charge residing in the exclusion zone.[7] The following elementary calculation shows that this interpretation is unphysical, because such concentrations of net charge would yield a vastly larger potential difference between the region exterior to the concentrated proton zone and the gel surface than the value actually measured. The gel surface is imagined to be an infinite vertical plane (i.e., containing the laboratory z-axis), whose outward normal is directed along the x-axis, as indicated in Figure 1. The gel surface is positioned at $x = 0$. The exclusion zone (region 1) extends from $x = 0$ to $x_1 = 200$ μm, and has infinite extent in the other two (y and z) dimensions. The proton zone (region 2) extends from $x_1 = 200$ μm to $x_2 = 2200$ μm, and also has infinite extent in the other two dimensions. This positive zone has width $x_2 - x_1 = 2$ mm and corresponds to the region of highest (apparent) proton concentration ($\geq 10^{-3}$ M) in Figure 1B of ref 7. Under the Pollack interpretation, the proton concentration in the proton zone is the concentration of net positive elementary charges, and is here conservatively set to the lower limit of 10^{-3} M, which yields a charge density of $\rho_2 = 9.65 \times 10^4$ C/m^3 in region 2. The residual net charge in the 10-fold smaller region 1 must cancel that of the proton zone, so its charge density must be 10-fold greater; hence, $\rho_1 = -\rho_2(x_2 - x_1)/x_1 = -9.65 \times 10^5$ C/m^3 in region 1. The one-dimensional Poisson equation of electrostatics, $\partial^2\phi/\partial x^2 = -(1/\varepsilon\varepsilon_0)\rho(x)$, where $\varepsilon = 80$ is the relative dielectric constant and $\varepsilon_0 = 8.85 \times 10^{-12}$ F/m is the permittivity of free space, is solved for this model of two adjacent slabs of uniform charge density with equal and opposite total charge to obtain the electrostatic potentials $\phi_1(x)$ and $\phi_2(x)$ in regions 1 and 2, respectively. The boundary conditions—$\phi_2(x_2) = 0$, $\partial\phi_2(x_2)/\partial x = 0$, $\phi_2(x_1) = \phi_1(x_1)$, and $\partial\phi_1(x_1)/\partial x = \partial\phi_2(x_1)/\partial x$—were applied to obtain the final results: $\phi_1(x) = -(\rho_1/2\varepsilon\varepsilon_0)(x^2 - x_1x_2)$ and $\phi_2(x) = -(\rho_2/2\varepsilon\varepsilon_0)(x - x_2)^2$. For the charge densities indicated above, the potential at $x = 0$ is $\phi_1(0) = -3.0 \times 10^8$ V, which exceeds the maximum experimental value, −0.2 V, by a factor of 1.5×10^9! The electric field at $x = x_1$ is $\mathbf{E} = -\partial\phi(x_1)/\partial x = (\rho_1/\varepsilon\varepsilon_0)x_1 = 2.7 \times 10^{11}$ V/m $= 2.7 \times 10^9$ V/cm, which exceeds by ~9000-fold the value ($\sim 3 \times 10^5$ V/cm) required for dielectric breakdown of water by 0.06 μs pulses.[23] Evidently, the 10^{-3} M H^+ concentration in the proton zone overestimates by (1.5×10^9)-fold any charge density that might actually be present, so the vast majority of those H^+ ions (all but ~1 in 1.5×10^9) must be accompanied by negative counterions! The net charge density in the exclusion zone must similarly be reduced by the same factor (1.5×10^9) in order to yield a predicted voltage matching the measured value, 0.2 V. (As noted earlier, the measured voltage does not necessarily require *any* net charged zones in the solution when ion concentrations at $x = 0$ and $x = x_2$ differ sufficiently.) It is now obvious that practically all protons in the proton zone did not originate in the exclusion zone but instead must have emerged *along with their counterions* from the Nafion and passed jointly through the exclusion zone. Such behavior flatly contradicts any claim that the exclusion zone contains no mobile charges.

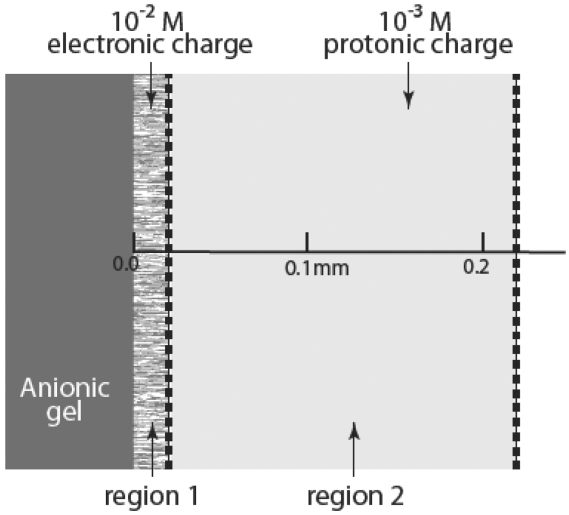

Figure 1. Schematic diagram of the model charge distribution employed in the electrostatic potential calculation. The x-axis is that shown in the figure. Each region (anionic gel, region 1, and region 2) is assumed to have finite extent in the x-direction but infinite extent in the plane normal to that. Region 1 extends from 0 at the gel−solution interface to 0.02 cm, and region 2 extends from 0.02 to 0.22 cm. The concentration of negative (electronic) charges in region 1 is 10^{-2} M, and the concentration of positive (protonic) charges in region 2 is 10^{-3} M.

Pollack and co-workers have repeatedly interpreted pH measurements, whether by indicator dyes or pH microelectrodes, as direct indications of the concentration of excess positive charges (H^+, pH < 7.0) or excess negative charges (OH^-, pH > 7.0) in violation of the usual constraint of electroneutrality over macroscopic regions.[6,7,24] In one case, the gradients of H^+ and OH^- were associated not with ionic gel or ionomer surfaces but instead with platinum anodes or cathodes, respectively, when electric current was driven through "pure" water by a 2.5−4.0 V potential difference.[24] The regions of excess H^+ and OH^- in these experiments were attributed to long-lived immobile positive and negative charges in separate regions of differently ordered water, which were proposed to exhibit "structural networks that have mirror symmetry to one another".[24] The water in these two different macroscopic regions was claimed to be charged by the passing current in rough analogy with the charging of a capacitor.[24] However, Corti and Colussi (CC)[25,26] pointed out that all observations of Ovchinnikova and Pollack[24] (OP), including those pertaining to slow discharging in the absence of an external electromotive force, could be quantitatively rationalized without violating electroneutrality by assuming that water was simply electrolyzed during the "charging" step, which thereby creates a concentration cell. The "discharging" process proceeds very slowly by diffusion of all species and loss of H_2(gas) and O_2(gas) to the atmosphere and, in the closed circuit case, also by the reverse of the hydrolysis process.

In their response to this prosaic alternative explanation of their results, OP attacked the "principle of electroneutrality

dx.doi.org/10.1021/jp302589y | J. Phys. Chem. B 2013, 117, 7653−7674

invoked by CC", and stated: "Exactly where this principle originated is unclear, but violations can be found at levels ranging from the atomic to cosmic."[27] In fact, this principle pertains only to systems of macroscopic extent with a significant concentration of mobile charge carriers that are either *at or near thermodynamic equilibrium*. It arises because the electrostatic free energy of any macroscopic region rises so rapidly with net charge that any configurations of the mobile ions that exhibit significantly charged macroscopic regions are far less probable than configurations that are closer to macroscopic electroneutrality. In addition, such configurations cannot be maintained for more than brief moments in water, because their mobile ions respond to the self-electric field of such configurations by Ohmic conduction, which typically proceeds far more rapidly than diffusion. The normal modes of the macroscopic dynamical transport equations for ions in solution (which include ion migration in internal electric fields arising from electroneutrality violations) are spatially periodic Fourier modes, each of which is a linear combination of the corresponding Fourier components of the concentrations of the individual ion types with the same period.[28−31] For a system containing n_c electroneutral components and $n_c + 1$ kinds of ions, there are always n_c electroneutral normal modes of a given period, l, which relax diffusively, and a single charged normal mode that relaxes rapidly primarily by Ohmic conduction.[28−31] The mean-squared amplitude of a charged mode with period l varies as l^{-2} and vanishes in the long-wavelength limit, $l \rightarrow \infty$.[31] In other words, periodic spontaneous fluctuations due to electroneutrality violations in the long-wavelength limit at room temperature are so small as to be invisible.

It is illuminating to calculate the electrostatic free energy of the combined exclusion and proton zones that were discussed above. In general, the electrostatic free energy of a fixed distribution of charges is given by

$$G^{el} = 1/2 \int d^3\mathbf{r} \int d\rho(\mathbf{r})\phi(\mathbf{r}) \tag{10}$$

When these integrals are performed over subvolumes of regions 1 and 2 with 1.0 × 1.0 cm^2 cross sections in a plane perpendicular to x, the electrostatic free energy of the net neutral 1.0 × 1.0 × 0.22 = 0.22 cm^3 subvolume comprising a negative slab of 0.02 cm thickness with 0.01 M OH^- and a positive slab of 0.2 cm thickness with 0.001 M H^+ is $G^{el} = 1.99 \times 10^6$ J. This G^{el} exceeds the latent heat to vaporize all of the water molecules in the 0.22 cm^3 volume, namely, $\Delta H_{vap} = 538$ J, by 3699-fold. Thus, the electrostatic free energies associated with excess ion densities of 0.01 or 0.001 M in regions 1 and 2 far exceed the energy required to vaporize the solution, and could not be observed, except as an extremely short-lived transient state.

We now suggest that the potentials associated with exclusion zones arise from gradients of one or more *electroneutral* ionic solutes in the region exterior to the gel, and can be regarded as long-range liquid junction potentials between the solution at probe position $\mathbf{R}_2$ in the gradient and that at reference position $\mathbf{R}_1$ at a very large distance from the gel, where the gradient has practically vanished. The ion gradients are assumed to be normal to the gel surface, and the positions $\mathbf{R}_1$ and $\mathbf{R}_2$ are here assumed to lie on the same surface normal.

The experimental situation is indicated schematically in Figure 2. Each electrode is immersed in a solution with a gradient of a dilute ionic solute. Consider first the electrode near $\mathbf{R}_1$. KCl diffuses out of the 3.0 M KCl internal reservoir to

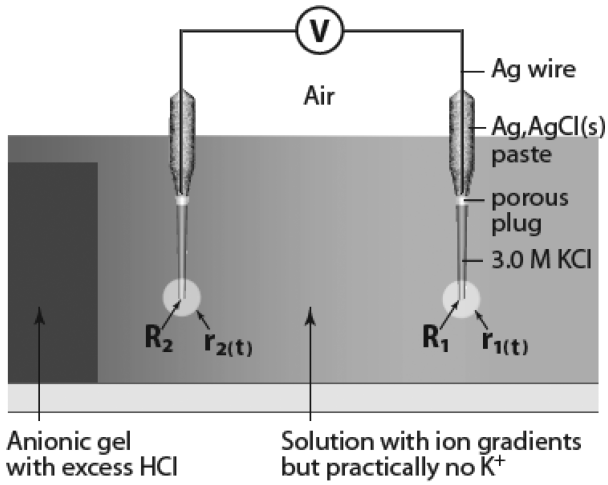

Figure 2. Schematic diagram of electrochemical electrodes used for calculation of long-range liquid-junction potential. The solution contains a gradient of one or more ionic components that do not contain K^+. A small spherically symmetric plume of KCl diffuses out from the tip of each electrode, which contains an internal reservoir of 3.0 M KCl. The conductance is dominated by KCl from the surfaces of the Ag wires, where the reversible half-cell reactions occur, to spherical surfaces of positions denoted by $\mathbf{r}_1(t)$ and $\mathbf{r}_2(t)$ in the KCl plume. The conductance along any path external to those spherical surfaces is dominated by ions of the solution gradient. The distance $|\mathbf{r}_2(t) - \mathbf{r}_1(t)|$ is assumed to far exceed $|\mathbf{r}_1(t)|$ and $|\mathbf{r}_2(t)|$, which are assumed to be very similar in magnitude.

create a very small plume of KCl in the adjacent solution. The total potential change accompanying a small electrical current flow from position $\mathbf{R}_1$ at the end of the internal KCl reservoir of the reference electrode to position $\mathbf{R}_2$ at the end of that of the probe electrode at a given time t is given by the line integral[32]

$$\begin{aligned}\mathcal{E}(t) &= \psi(\mathbf{R}_2, t) - \psi(\mathbf{R}_1, t) \\ &= -(RT/F) \int_{\mathbf{R}_1}^{\mathbf{R}_2} \Big(\sum_\alpha t_\alpha(\mathbf{r}, t) \nabla \ln[c_\beta(\mathbf{r}, t)]\, d\mathbf{r} \\ &\quad - \sum_\beta t_\beta(\mathbf{r}, t) \nabla \ln[c_\beta(\mathbf{r}, t)]\, d\mathbf{r} \Big)\end{aligned} \tag{11}$$

where the sum on α runs over all cations, β runs over all anions, and $t_\alpha(\mathbf{r}, t)$ or $t_\beta(\mathbf{r}, t)$ denotes the position-dependent transference number (i.e., fraction of the current carried by the indicated ion at time t at point $\mathbf{r}$) along the path from $\mathbf{R}_1$ to $\mathbf{R}_2$. The transference number is given by $t_\alpha = c_\alpha z_\alpha^2 D_\alpha / (\sum_\gamma c_\gamma z_\gamma^2 D_\gamma)$, where γ runs overall ions, z_γ is the ion valence, and D_γ is its diffusion coefficient. This line integral can be shown to be independent of path from $\mathbf{R}_1$ to $\mathbf{R}_2$. An illuminating approximate evaluation is made by assuming the following:

(a) KCl dominates the conductance from $\mathbf{R}_1$ to a surface of positions $\mathbf{r}_1(t)$ in the KCl plume around the $\mathbf{R}_1$ electrode and from $\mathbf{R}_2$ to a surface of positions $\mathbf{r}_2(t)$ in the KCl plume around the $\mathbf{R}_2$ electrode.

(b) A single electrolyte, $S = X^+ + Y^-$, which is not KCl, dominates the conductance along any path from any of the $\mathbf{r}_1(t)$ positions to any of the $\mathbf{r}_2(t)$ positions.

(c) The size of the plumes is sufficiently small compared to $|\mathbf{R}_2 - \mathbf{R}_1|$ that the exact choice of $\mathbf{r}_1(t)$ and $\mathbf{r}_2(t)$ has a negligibly small effect on the computed potential change from $\mathbf{r}_1(t)$ to $\mathbf{r}_2(t)$. Consequently, the potential change from $\mathbf{R}_1$ to $\mathbf{R}_2$ varies only weakly as the plume evolves in time.

dx.doi.org/10.1021/jp302589y | J. Phys. Chem. B 2013, 117, 7653−7674

In view of assumption a, the KCl contributions from $\mathbf{R}_1$ to $\mathbf{r}_1(t)$ and from $\mathbf{r}_2(t)$ to $\mathbf{R}_2$ cancel except for a very small contribution arising from the fact that $|\mathbf{R}_1 - \mathbf{r}_1(t)|$ slightly exceeds $|\mathbf{R}_2 - \mathbf{r}_2(t)|$ when $c_S(\mathbf{r}_2, t) > c_S(\mathbf{r}_1, t)$, because $\mathbf{r}_2(t)$ must be slightly closer to its 3.0 M KCl reservoir to attain dominance of KCl under those conditions. This small contribution is ignored here. In the region from $\mathbf{r}_1$ to $\mathbf{r}_2$, the conductance is (by assumption b) dominated by dilute S, so $c_{X^+} = c_{Y^-} = c_S$, and the transference numbers are constants independent of $\mathbf{r}$ or t. In this event, the non-canceling part of the potential is given by

$$\begin{aligned}\mathcal{E}(t) &= -(RT/F)(t_{X^+} - t_{Y^-}) \int_{\mathbf{r}_1(t)}^{\mathbf{r}_2(t)} \nabla \ln[c_S(\mathbf{r}, t)]\, d\mathbf{r} \\ &\cong -(RT/F)(t_{X^+} - t_{Y^-})(\ln[c_S(\mathbf{r}_2(t), t)] \\ &\quad - \ln[c_S(\mathbf{r}_1(t), t)]) \\ &\cong -(RT/F)(t_{X^+} - t_{Y^-}) \ln[c_S(\mathbf{R}_2)/c_S(\mathbf{R}_1)] \qquad (12)\end{aligned}$$

where, in the last line, the position of each electrode tip ($\mathbf{R}_1$ or $\mathbf{R}_2$) has been substituted for the position ($\mathbf{r}_1(t)$ or $\mathbf{r}_2(t)$) in its plume, where dominance of the conductance switches from KCl to S. This is a good approximation whenever the plume size and $|\nabla \ln[c_S(\mathbf{r}, t)]|$ are sufficiently small that $\ln[c_S(\mathbf{r}, t)]$ remains essentially constant over the distances $|\mathbf{r}_1(t) - \mathbf{R}_1|$ and $|\mathbf{r}_2(t) - \mathbf{R}_2|$, and that $\mathbf{r}_2(t) - \mathbf{r}_1(t)$ is very nearly parallel to $\mathbf{R}_2 - \mathbf{R}_1$.

Apart from the transference factor, eq 12 has the form of the potential of a concentration cell. When the electrolyte is S = H^+ + Cl^-, which is most likely the case in some of the examples reported by Pollack and co-workers, then $t_{H^+} - t_{Cl^-} \cong (D_{H^+} - D_{Cl^-})/(D_{H^+} + D_{Cl^-}) = 0.75$ at 298 K. Then, if $c_{HCl}(\mathbf{r}_2, t) > c_{HCl}(\mathbf{r}_1, t)$, which will be the case whenever the gradient of HCl is inward, as expected when HCl is released from the Nafion or negatively charged gel, the potential will be negative and increasing in magnitude as the probe electrode at $\mathbf{R}_2$ is moved closer to the gel surface. For example, if $\mathbf{R}_2$ is near the Nafion surface and if $c_{HCl}(\mathbf{R}_2)/c_{HCl}(\mathbf{R}_1) = 1435$, then, at 298 K, $\mathcal{E} = -140$ mV, which is comparable to the voltage measured with the probe electrode close to the Nafion surface.[2,3,9] A 1435-fold ratio of HCl concentrations corresponds to a pH difference of ~3.2, which lies within the reported range of pH variation along a normal to the surface of a Nafion membrane.[7] Potential measurements were also reported for both (negatively charged) cation exchange and (positively charged) anion exchange gel beads in 10 mM imidazole (Im + $ImH^+ \cdot Cl^-$) buffer.[5] However, in the former case, at least three kinds of ions (H^+, ImH^+, and Cl^-) and in the latter at least four kinds of ions (Na^+ (or other monovalent cation), OH^-, Cl^-, and ImH^+) must be taken into account in eq 11. In the absence of quantitative concentration profiles for each kind of ion in the steady state, quantitative evaluation of the steady-state potential, $\mathcal{E}(t)$, cannot be achieved, and is not undertaken here.

Potentials measured near a Nafion membrane in 1 mM solutions of different alkali chloride salts exhibited different curves of potential versus distance.[2] In each case, the potential was negative, but its magnitude increased in the order $Li^+ \rightarrow Na^+ \rightarrow K^+$. A large inward gradient of HCl is expected due both to release of excess HCl from the Nafion and to exchange of alkali cations in the solution for protons in the Nafion. Protons likely dominate the solution transference due to their very large diffusion coefficients. Hence, the primary effect of the alkali cations likely stems from their ability to exchange with protons and thereby increase the HCl concentration at the membrane surface and thus enhance the inward HCl gradient. If the exchange rate were to increase in the order $Li^+ \rightarrow Na^+ \rightarrow K^+$, that would account qualitatively for the observations. A measurement of exchange rates of well-stirred 0.1 M solutions of LiCl, NaCl, KCl, RbCl, and CsCl with a Nafion membrane, which was pretreated by equilibration with 0.1 M HCl, gave exchange rates that increased monotonically with increasing atomic number, except for K^+, which exchanged at the same rate as Na^+.[33] However, it was recognized that such measurements were sensitive to the state of the membrane, for example, to hydration, which could be significantly greater in the 0.001 M salt solutions studied by Zheng et al.[2] In fact, the results of Zheng et al. could be taken as evidence that 1 mM K^+ exchanges more rapidly than 1 mM Na^+, which in turn exchanges more rapidly than 1 mM Li^+ under the prevailing conditions.

In summary, the electrochemical potentials reported by Pollack and co-workers most likely arise from the same long-range electrolyte (acid/base and/or salt) gradients that provide the chemotactic forces responsible for the exclusion zones. With sufficiently detailed information regarding the concentrations of electroneutral ionic components as a function of distance from the surface of a neutral or charged gel, the potential could be accurately reckoned as a function of probe position using eq 6. Comparison of that estimate with the measured values would provide an important quantitative test of this proposed origin of the long-range potentials.

III. Infrared Imaging. An image of the upward spontaneous (thermal) infrared (IR) emission in the spectroscopic wavelength window, 3.8−4.6 μm, from a strip of Nafion and its surrounding water was reported.[2] It was not specified whether the top surface of the Nafion was submerged beneath, or protruded above, the surface of the surrounding bulk water. The emission above the Nafion strip was indistinguishable (in intensity) from that above the bulk water, whereas much darker zones of width 300−500 μm were observed along the interfaces between the lateral surfaces (or edges) of the Nafion and the bulk water and were attributed to ordered water with reduced IR emissivity. However, this explanation is not consistent with the reported IR image unless unlikely special conditions are met, as described below.

IR emission of liquid water in the 4.0−4.6 μm wavelength range comes essentially entirely from the region within 60 μm of the air−water interface for the following reason. Analysis of the emission intensity as a function of water film thickness yielded absorption lengths of L = 23−15 μm over this wavelength range.[35] L is the distance over which the intensity of incident radiation falls to e^{-1} of its initial value. L also can be estimated from the reported imaginary refractive index, k = 0.018, for λ_0 = 4.6 μm,[20] which yields, $L = \lambda_0/(4\pi k) = 0.0020$ cm = 20 μm. This agrees reasonably well with the value (15 μm) derived from emission measurements, and confirms that practically none of the emission orginates from a depth greater than 60 μm. Unfortunately, important dimensions in the experiments of Zheng et al. such as thickness of the Nafion sample and depth of the bulk water were not specified.[2]

If the Nafion surface is assumed to induce long-range ordered water with greatly reduced emissivity, then the top surface of a deeply submerged Nafion should be overlain by a slab of such ordered water with a thickness equal to the width (w = 300−500 μm) of the ordered water zones adjacent to its lateral surfaces. If the depth of the water above the Nafion exceeds (w + 60) μm, then the IR emission above both the

dx.doi.org/10.1021/jp302589y | J. Phys. Chem. B 2013, 117, 7653−7674

Nafion and the lateral ordered water zones should match that of the bulk water, contrary to observation. If the depth of the water above the Nafion is reduced into the range (60 to (60 + w)) μm, where emission can originate in the putative ordered water atop the Nafion, then the emission above the Nafion should be less than that above the bulk water, contrary to observation. For such water depths, the emission above the Nafion should also be less than that above the lateral ordered water zones, which extend normal to the edges of the Nafion and lie farther below the surface, again contrary to observation. For still smaller water depths, 0−60 μm, above the top Nafion surface, some of the emission above the Nafion originates in the Nafion itself, whose emissivity almost certainly differs from that of either bulk water or the putative ordered water. Only if the emissivity of the Nafion were to exceed that of the bulk water by just the right amount would the emission above the Nafion match that of the bulk water. Because this "right amount" depends strongly upon the actual water depth above the Nafion in this 0−60 μm range, the range of water depths that could yield similar emission to that of the bulk water for any given Nafion emissivity is at most a small fraction of the interval 0−60 μm. The *a priori* probability that the actual water depth above the Nafion lies within this small fraction of that interval is rather small, so this possibility is rather unlikely. The remaining possibility is that the top surface of the Nafion lies above that of the water. In this case, the emissivity of the Nafion would have to match that of the bulk water in order to yield the reported image, which again is most unlikely. Consequently, the proposed long-range ordered water with reduced emissivity is for any water depth either incompatible with the reported image or requires an unlikely circumstance in order to be compatible with that. Without knowledge of the actual water depth atop the Nafion and the emissivity of Nafion relative to bulk water, the IR image does not constitute unambiguous evidence for long-range ordered water. Moreover, when such information becomes available, the IR image could well rule out the ordered water hypothesis.

There appears to be only three ways for any given region of the surface to radiate less thermal energy in the vertical direction than its neighboring regions: (1) the local temperature is lower than elsewhere, (2) its top 60 μm is less emissive than elsewhere due to a different composition or structure, or (3) the normal to the surface is not vertical. If the top surface of the Nafion protrudes above that of the surrounding solution, as illustrated in Figure 3a, then all three possibilities might apply. The convex curvature of the wetting water, as it bends downward from the top surface to the sidewall at the edge of the Nafion, would provide a greater vapor pressure and evaporation rate in that region than elsewhere, which in turn would lead to a greater local cooling rate and a greater local rate of accumulation of any less emissive surface-active compounds emanating from the Nafion. Moreover, the normal to the wetting water surface tilts away from vertical, as the wetting water bends downward, and does not return to vertical until this meniscus has flattened out at the level of the bulk solution. The intensity of thermal IR emission from water decreases slightly with increasing angle from the surface normal up to 40°, and declines significantly beyond 45°.[36] When the surface normal is tilted by θ from the vertical, vertical emission perforce makes the same angle, θ, with respect to the surface normal. Thus, significantly decreased vertical emission is expected for a meniscus surface, whose normal is tilted from vertical by $\theta \geq 45°$.

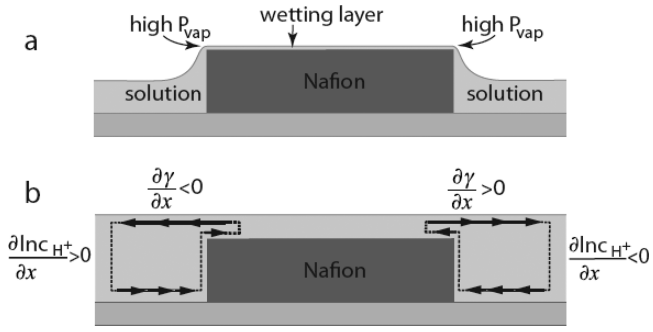

Figure 3. Possible alternative explanations for decreased intensity of upward emission of thermal IR radiation, from the region near the Nafion−water boundary. (a) If the Nafion protrudes above the surface of the adjacent bulk water, reduced emission could result from a sufficiently tilted meniscus surface, local cooling due to a higher equilibrium vapor pressure and evaporation rate in the region of maximum convex curvature, or concentration of less emissive surface active species emanating from the Nafion due to evaporative loss of water at the point of maximum convex curvature. (b) If the Nafion is completely submerged, the top surface of the solution above the Nafion edge might be selectively enriched in less emissive surface-active species, or significantly cooled, by the convection cell indicated. Such convection might be driven by a combination of inward chemotactic forces exerted by the glass bottom on the solution, which contains an outward OH^- gradient, or by outward Marangoni convection of the top surface due to an outward gradient of surface tension, possibly arising from an inward concentration gradient of surface-active species emanating from the Nafion. The cooling of solution adjacent to the Nafion could occur as a consequence of endothermic H_2O uptake and swelling.

In order to attain a tilt angle of $\theta \geq 45°$ over a horizontal distance of 300−500 μm, the Nafion sample would have to protrude above the surrounding water by at least a comparable distance.[37] If the sample was actually a strip of Nafion 117, then its dry thickness is ∼180 μm, so it would have to be swollen by a factor of 2 or more in order to achieve a 300−500 μm wide dark zone, which seems rather unlikely. Thus, if the sample was a flat strip of Nafion 117 that protruded above the level of the surrounding water, then local cooling and/or accumulation of less emissive compounds in the most convex regions of the wetting film are plausible alternative explanations for the dark zones that have not yet been ruled out.

If the top surface of the Nafion lies below that of the solution, then a level surface is expected. However, local cooling might still be possible provided that the process of H_2O uptake and swelling of the Nafion is endothermic. In fact, uptake of H_2O and swelling of the Nafion increases with temperature, so that process must be endothermic. In the absence of convection, the solution surface above the edges of the Nafion would not be cooler than in the center of the film. However, the released acid generates an inward horizontal gradient of c_{H^+} in the solution. It was predicted and shown in paper I (10.1021/jp302587d) that, when a solution bearing a pH gradient is in contact with a negatively charged glass surface, a chemotactic force on the solution induces convection in the direction of greater acidity. A similar conclusion applies as well to a Nafion surface. As a consequence of such convection and its associated back-flow, a convection pattern like that in Figure 3b is expected. This flow pattern may also be reinforced or even dominated by Marangoni convection of the top layer in the $+x$ direction, which could arise from a gradient of the surface tension, which in turn could be due to the gradient of any

compounds emanating from the Nafion that adsorb to the interface. In such a case, the surface tension is lower above the Nafion than elsewhere, so the top layer of the solution is pulled outward from the region above the edges of the Nafion, thereby expanding the low tension region at the expense of the high tension region. In such an event, the surface experiences a traction in the direction of $\partial\gamma/\partial x$, which must be balanced by a viscous traction in the opposite direction due to a shear gradient, $\partial v_x/\partial z$, of the x-component of the velocity of the underlying solution. Hence, in the region where $\partial\gamma/\partial x > 0$, $\partial v_x/\partial z$ must be positive, and the maximum induced positive v_x is found at the top surface (air−water interface). The resulting convection cell would bring cooled solution (caused by heat absorption accompanying the Nafion swelling process) from the wall of the Nafion edge up to the top surface much more rapidly than could be achieved by thermal diffusion. In this way, cool solution could be transported upward before heat could diffuse in laterally. This would effectively increase the area available for cooling the solution above the Nafion edge without increasing the horizontal projection (nearly zero) of that surface, and that in turn should provide a significantly cooler patch of surface above the Nafion edge than elsewhere. Thus, if the top surface of the Nafion should lie below that of the bulk solution, this is a plausible alternative explanation for the dark zones that has not yet been ruled out.

IV. NMR Imaging. A sample consisting of a cylindrical plug of 10% poly(vinyl alcohol) gel in the lower part of an NMR tube with bulk water on top was examined by magnetic resonance T_2 imaging of the water protons.[2] At low resolution, when the pulsed magnetic field imaging gradients were small, "the apparent T_2 in the gel phase was substantially shorter than that in the bulk water phase". This circumstance implies that the transverse magnetization of water protons (in the rotating frame) dephased more rapidly in the gel than in the bulk water. Most likely, this was due to translational diffusion of water in the gel through, and chemical exchange with water in, regions of different magnetic susceptibility that exhibit slightly different local magnetic field strengths and Larmor frequencies. At the higher resolution (~20 μm) required to resolve the interfacial region, the pulsed magnetic field gradients were much greater, and the now much shorter apparent T_2 (30.2 ± 0.3 ms) of the gel phase slightly exceeded that of the bulk water (27.2 ± 0.3 ms). The change in the T_2 (gel)/T_2(bulk water) ratio from substantially less than 1.0 in small magnetic field gradients to slightly greater than 1.0 in large gradients can be rationalized in the following way. When the pulsed magnetic field gradients are so large (as required for 20 μm resolution), they typically dominate the intrinsic variations in the local magnetic field. In this case, dephasing of the transverse magnetization by translational diffusion proceeds far more rapidly than in weak or vanishing gradients. The observed ratio, T_2(gel)/T_2(bulk water) = 1.1, implies that translational diffusion of water is on average slower in the 10% PVA gel than in the water, presumably due to partial obstruction by gel fibers and/or occasional occupation of stationary sites. Consequently, in any time interval, water molecules in the gel sample a smaller region of the pulsed magnetic field gradients than do those in bulk water, and dephase their transverse magnetization to a lesser extent, which results in a larger apparent T_2. In the high resolution image, a zone of ~10% lower T_2 (25.4 ± 0.2 ms) than that of bulk water was observed along the apparent gel−water interface. This T_2 presumably applies to a voxel of 20 μm height (the stated resolution) that either straddles or is adjacent to the gel−water boundary. The width of this interfacial zone was stated to be 60 μm, which presumably is spanned by three voxels, but whether all three voxels exhibited precisely the same value of T_2 was not stated. This interfacial zone was attributed to ordered water extending outward from the gel surface into the bulk water. In any case, the lower T_2 of the interfacial zone compared to that of bulk water implies either a *greater* water diffusion coefficient or a greater heterogeneity of the magnetic susceptibility and local magnetic field in the interfacial zone, or both.

Pulsed field gradient spin−echo measurements of water self-diffusion parallel to the interface in a slice containing the interface were performed at the same 20 μm resolution. The effective diffusion coefficient was presumably extracted in the standard way from the increase in the irreversible dephasing rate with increasing strength and/or duration of the gradient pulses that provide the diffusion-induced phase shifts on either side of the 180° pulse of the diffusion spin echo sequence. Diffusion was reported to be slightly slower "in the gel phase than in the bulk water phase", and in the interfacial zone was "substantially different from either the bulk water or gel phases", but neither quantitative values nor the direction of the difference were specified. However, it was concluded that "water molecules at the interface suffer appreciable restriction". From this comment, one could reasonably infer that the rate of dephasing of the transverse magnetization (in the rotating frame) increased less rapidly with increasing strength and/or duration of the pulsed gradients of the diffusion spin echo sequence in the interface than is the case in either the bulk water or gel.

If we assume that heterogeneity of the susceptibility and local magnetic field make no significant contribution to the dephasing of transverse magnetization in the interfacial region, then the diffusion imaging results imply a *lower* effective diffusion coefficient in the interfacial region than that of bulk water, whereas the relative T_2 values of the interfacial and bulk water regions imply a *greater* diffusion coefficient in the interfacial region. This contradiction precludes any explanation of the interfacial zone that does not involve significant heterogeneity of the local magnetic susceptibility in the interfacial region! Thus, the conclusion of Pollack and co-workers that the interfacial zone consists of homogeneous ordered water with a reduced diffusion coefficient cannot by itself provide a satisfactory explanation of the combined T_2 and diffusion image data.

Consider now a possible alternative explanation of the NMR results, wherein (i) water diffusion in the interfacial zone is the same as that in bulk water and only slightly faster than that in the gel and (ii) the difference in (average) magnetic susceptibility between the bulk water and the gel is taken into account. The volume susceptibility of the 10% PVA gel apparently has not been measured but is here estimated approximately by $\chi(\text{gel}) = (0.1)\chi(\text{EtOH}) + 0.9\ (\chi_{H_2O})$, where EtOH denotes ethanol, $\chi(\text{EtOH}) = -7.29 \times 10^{-6}$, and $\chi(H_2O) = -9.04 \times 10^{-6}$ in SI units. The difference in susceptibility between the gel and bulk water is then $\Delta\chi \equiv \chi(\text{gel}) - \chi(H_2O) = (0.1)(\chi(\text{EtOH}) - \chi(H_2O)) \cong +1.75 \times 10^{-7}$ (SI units), and the corresponding difference in Larmor angular frequency between the gel and water is $\Delta\omega \equiv \omega(\text{gel}) - \omega(\text{water}) = 2\pi\nu_0\Delta\chi = +550$ rad s^{-1}, where $\nu_0 = 500 \times 10^6$ Hz is the precession frequency of protons in the main magnetic field of a 500 MHz spectrometer. As will be seen, this difference in

dx.doi.org/10.1021/jp302589y | J. Phys. Chem. B 2013, 117, 7653−7674

Larmor frequency suffices to significantly dephase the transverse magnetization of those water molecules that initially reside in one phase (gel or bulk water) but in the course of their translational diffusion cross the water−gel boundary at least once and spend sufficient time in the other phase, as illustrated in Figure 4.

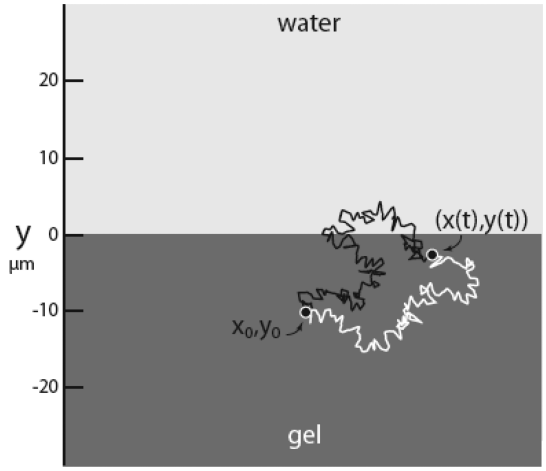

Figure 4. Illustration of two possible Brownian paths that begin at the same point (x_0, y_0) and end at the same point $(x(t), y(t))$ at time t. Imaging magnetic field gradients are applied in the vertical (y) direction. In some experiments, diffusion field gradients are also applied in the horizontal direction. Because the bulk susceptibility differs significantly in the two phases, the Larmor frequency of the protons in a water molecule changes when it crosses the gel−water boundary. Consequently, those protons accumulate an additional phase difference relative to that of stationary water, in addition to that due to diffusion in the applied magnetic field gradients. Such cross-boundary diffusion acts to decrease the apparent T_2 of those water molecules that cross the boundary within time T_2. It also lowers the rate at which dephasing of the magnetization increases with increasing strength or duration of the diffusion gradient pulses, and that in turn causes a decrease in the apparent diffusion coefficient, as described in the main text.

We now focus on those molecules of the bulk water that lie at a distance y_0 from the water−gel boundary at $t = 0$, when their magnetization is tilted into the xy plane of the rotating frame. For simplicity, the diffusion coefficient of water is here taken to be the same in both gel and bulk water phases. Also, the initial position of the water molecules is taken to be $y = 0$, and the water−gel boundary is at $y = y_0$. The fraction of these water molecules in the gel phase at time t is found from standard diffusion theory to be

$$P(y \geq y_0, t) = \int_{y_0}^{\infty} dy \exp[-y^2/4Dt]/(4\pi Dt)^{1/2} = (1/2)\,\mathrm{erfc}[y_0/2\sqrt{Dt}] \quad (13)$$

The time-average fraction of these molecules, which were initially at $y = 0$ in the aqueous phase, that are found in the gel phase over the time from 0 to t is

$$\langle P\rangle_t \equiv (1/t)\int_0^t dt P(y > y_0, t) = (1/t)\int_0^t dt(1/2)\,\mathrm{erfc}[y_0/2\sqrt{Dt}] = z_0^{\,2}\int_{z_0}^{\infty}(1/z^3)\,\mathrm{erf}[z]\,dz \quad (14)$$

where $z_0 \equiv y_0/2(Dt)^{1/2}$. $\langle P\rangle_t$ is equivalent to the average fraction of the time from 0 to t that each molecule (initially at a distance y_0 from the gel−solution boundary) spends on the other (gel) side of that boundary. Similar considerations apply to water molecules that are initially in the gel phase but cross to the aqueous phase, as indicated in Figure 4. $\langle P\rangle_t$ varies with t and with the initial distance y_0 from the gel−solution boundary, and can be further averaged over any range of y_0, such as $y_1 \leq y_0 \leq y_2$, according to $\langle\langle P\rangle_t\rangle_{y_1,y_2} \equiv (1/(y_1 - y_2))\int_{y_1}^{y_2} dy_0 \langle P\rangle_t$. After introducing $z_i \equiv y_i/(2(Dt)^{1/2})$, $i = 1, 2$, and integrating by parts, we obtain

$$\langle\langle P\rangle_t\rangle_{y_1,y_2} = (1/(z_2 - z_1))(1/3) \times \{z_2^{\,3}\int_{z_2}^{\infty} dz(1/z^3)\,\mathrm{erfc}[z] - z_1^{\,3}\int_{z_1}^{\infty} dz(1/z^3)\,\mathrm{erfc}[z] + \int_{z_1}^{z_2} dz\,\mathrm{erfc}[z]\} \quad (15)$$

The average accumulated phase (or dephasing) at time t of those water molecules that were initially in the range from y_1 to y_2 from the gel−solution boundary is given by

$$\Delta\phi(y_1, y_2, t) = \langle\langle P\rangle_t\rangle_{y_1,y_2} t 2\pi\nu_0\Delta\chi \quad (16)$$

which depends upon the time t subsequent to the initial $\pi/2$ pulse. The maximum time available for diffusion before the signal is attenuated is approximately $t_0 \simeq T_2$, where $T_2 = 0.025$ s is the time for dephasing by all mechanisms to reduce the signal amplitude to $\exp[-1]$ times its value at $t = 0$. To gain some insight into the magnitude of dephasing caused by diffusion of water molecules across the gel−solution boundary, $\Delta\phi(y_1, y_2, t_0)$ is evaluated by numerical integration for six contiguous intervals spanning the distance from 0 to 30×10^{-4} cm from the boundary. The self-diffusion coefficient of water is $D = 2.1 \times 10^{-5}$ cm^2/s at 293 K. For the six intervals, $(y_1, y_2) = (0, 5)$, $(5, 10)$, $(10, 15)$, $(15, 20)$, $(20, 25)$, and $(25, 30)$ in units of 10^{-4} cm, the average accumulated phases at $t_0 = 0.025$ s are, respectively, $\Delta\phi(y_1, y_2, 0.025) = 4.67$, 1.89, 0.657, 0.189, 0.043, and 0.014 rad.

The average accumulated phase due to cross-boundary diffusion can be compared with the root-mean-square accumulated phase due to self-diffusion of water molecules in the (dominant) imaging magnetic field gradient in the y-direction. The distribution of $\delta\phi(t)$ at time t is Gaussian with width $\sigma_t = \langle\delta\phi(t)^2\rangle^{1/2}$, and at time $t_0 = T_2$, the average projection of water proton magnetization onto the $\delta\phi = 0$ axis (in the rotating frame) is

$$\langle\cos\delta\phi(t_0)\rangle = \exp[-\sigma_{t_0}^{\,2}/2] = \exp[-t_0/T_2] = \exp[-1.0] \quad (17)$$

This gives $\sigma_{t_0} = \langle\delta\phi(t_0)^2\rangle^{1/2} = \sqrt{2} = 1.414$ rad *due to this mechanism*. The $\Delta\phi(0.0, 5.0 \times 10^{-4}, 0.025) = 4.67$ rad due to cross-boundary diffusion of water molecules in the interval from 0 to 5×10^{-4} cm exceeds $\sigma = 1.414$ by 3.3-fold and would

dx.doi.org/10.1021/jp302589y | J. Phys. Chem. B 2013, 117, 7653−7674

substantially shorten the T_2 of those water molecules. The $\Delta\phi(5 \times 10^{-4}, 10 \times 10^{-4}, 0.025) = 1.89$ due to water molecules in the interval $(5-10) \times 10^{-4}$ cm exceeds $\sigma = 1.414$ by 1.34-fold, and would significantly shorten the T_2 of those molecules. With increasing distance of the interval from the boundary, the average dephasing, $\Delta\phi(y_1, y_2, 0.025)$, declines and finally falls to $\sim(0.03)\sigma$ for the interval $(20-25) \times 10^{-4}$ cm, in which case the effect of cross-boundary diffusion to shorten T_2 is rather modest. These considerations suffice to indicate the effects of cross-boundary diffusion on the T_2 of free-induction decays.

A far more sophisticated theoretical treatment would be required to accurately model the effect of water diffusion across the gel−solution boundary on a simple spin echo or on successive even echoes of a Carr−Purcell−Meiboom−Gill (CPMG) pulse sequence. Nevertheless, the preceding calculations suffice to show that the presence of a boundary between two regions with a plausible difference in magnetic susceptibility can lead to significant additional accumulated phase (dephasing) of water molecules that are initially 15−20 μm or less from the boundary in the time $t_0 = T_2 = 0.025$ s. The reported image reveals excess dephasing (relative to that in bulk water) in at most three 20 μm high (in the y-direction) voxels, which could be considered to span the intervals −30 to −10, −10 to +10, and +10 to +30 in units of 10^{-4} cm, all of which should be significantly dephased (compared to $\sigma = 1.414$ rad) by cross-boundary diffusion. This average dephasing significantly shortens T_2 compared to that of bulk water far from the interface. This conclusion is in qualitative, and potentially also quantitative, agreement with the T_2 imaging observations which yield an ∼10% lower average T_2 of the two or three voxels across the interface.

Taking the gel−water boundary into account also accounts qualitatively for the results of the diffusion imaging experiments, specifically for the lower rate of increase of the dephasing with strength and/or duration of the diffusion gradient pulses (with gradients parallel to the interface) in comparison to that in bulk water. Two basic notions are invoked. (1) The total dephasing contains two contributions, namely, (i) $\sigma = \langle\delta\phi^2\rangle^{1/2}$, due to diffusion in the pulsed gradient and (ii) $\Delta\phi(y_1, y_2, t)$ due to the average time spent by water molecules on the opposite side of the gel−solution boundary from their starting positions in the interval, $y_1 \le y \le y_2$. (2) σ increases with increasing strength or duration of the pulsed magnetic field gradients, which leads to a smaller apparent T_2 in bulk water and a smaller time, $t_0 \cong T_2$, in which a water molecule initially at y_0 can diffuse to the boundary. This reduction in t_0 decreases $P(y \ge y_0, t_0)$ and $\Delta\phi(y_1, y_2, t_0)$. The net result is that total dephasing (of the transverse magnetization of water protons in their rotating frame) does not increase as rapidly with strength or duration of the pulsed gradient for the three voxels extending from 30 μm below to 30 μm above the horizontal gel water boundary, as it does for voxels of similar size in the bulk water far from the interface. This prediction agrees qualitatively, and potentially also quantitatively, with the experimental observation. Notably, this interpretation does not require any difference in diffusion coefficient between water in the interfacial region and that in bulk water. This same qualitative explanation applies also to the recent measurements of the apparent self-diffusion coefficient of water in interstices between precipitated ion exchange gel beads or Nafion beads.[34]

Although a considerably more detailed theory would be required to ascertain whether this alternative explanation provides quantitative agreement with the NMR imaging data, the above discussion suffices to indicate that it is a plausible and likely alternative explanation of the NMR imaging data, which has not yet been ruled out.

DISCUSSION

Sections I−IV addressed two main issues: (1) serious problems encountered when the long-range ordered water hypothesis was compared with a variety of data from four very different kinds of experiments and (2) qualitative comparisons of alternative explanations with those same experimental data. In certain comparisons with experiment, the long-range ordered water hypothesis was either contradicted outright (cf. the observed attractions in Table 1), contradicted unless some additional alternative process (that by itself could account completely for the observations) was also taking place (cf. the analysis of NMR imaging data), or contradicted except in the event that an unknown experimental parameter lay in an *a priori* unlikely small fraction of its possible range (cf. the analysis of IR emission imaging data). Numerous experiments show that agarose gels are readily permeable to small ions, proteins, and nucleic acids, which flatly contradicts any claim that exclusion zones contain only immobile charges. The presence of mobile charges necessarily implies that any significant excess charge in the exclusion zone would be very rapidly neutralized (or equivalently screened) by Ohmic conduction. Thus, a long-lived, significantly charged exclusion zone could not exist over a distance greater than a few Debye screening lengths, which have a maximum value of 0.3 μm in any solutions studied in the Pollack lab. In contrast, the expected (and in some cases observed) long-range concentration gradients of electrolytes, including NaOH and HCl, in such unstirred solutions are consistent with a long-range liquid junction potential that requires no macroscopic violation of electroneutrality. Under the chemotactic theory, gradients of ln c_{NaOH}, ln c_{HCl}, and/or ln c_{salt} contribute to chemotactic forces on the microspheres, which are in qualitative agreement with the exclusion/attraction data in Table 1.

The chemotactic theory not only agrees qualitatively with practically all of the extant observations pertaining to microsphere motions but also provides a number of untested predictions that were noted in section I. Most importantly, it is in every case testable by various means, including measurement of the putative prevailing ion gradients.

The present explanation for slow inward microsphere motion in the region beyond the attraction or exclusion zones involves Marangoni convection driven by a surface tension gradient, but the surface-active agent(s) responsible for that gradient remain unidentified. Given the amphiphilic nature of the gel constituents, those are the most likely candidate surfactants. The same substance(s) could in principle also drive the Marangoni convection cell that is part of the alternative explanation for the thermal IR image.[2] Identification of this and any other surface-active species emanating from Nafion and from both kinds of ion exchange gel beads would be a valuable first step in assessing such alternative explanations.

CONCLUSION

The long-range ordered water hypothesis is confronted by many serious problems, including its contradiction by various experimental data and its strong violation of the principle of macroscopic electroneutrality. In practically every case, where it

dx.doi.org/10.1021/jp302589y | J. Phys. Chem. B 2013, 117, 7653−7674

has been invoked, plausible alternative explanations of the experimental data, which require no new properties or phases of water, no violations of electroneutrality or other established principles, and no new chemical or physical laws, have been proposed. Certain predictions of both the macromolecular chemotaxis theory, proposed to account for microsphere exclusion/attraction phenomena, and the long-range liquid junction potential theory, proposed to account for the measured electrostatic potentials, enable additional direct experimental tests in the future.

APPENDIX A. COMPOSITIONS OF POLY(ACRYLIC ACID) GELS IN EQUILIBRIUM WITH DIFFERENT BATHING SOLUTIONS

Polyacrylic acid contains weak acid groups (P−COOH). For the present qualitative purposes, it suffices to treat these groups as independent with pK = 6.0, which is the midpoint of the titration curve.[35] A dissociation reaction of a gel carboxyl group is

$$\mathrm{PCOOH} \rightleftharpoons \mathrm{PCOO^-} + \mathrm{H^+} \tag{A1}$$

with equilibrium constant[38]

$$K_d^g = \frac{c_{\mathrm{PCOO^-}} c_{\mathrm{H^+}}}{c_{\mathrm{PCOOH}}} = 10^{-6}\ \mathrm{M} \tag{A2}$$

The ionized fraction of carboxyl groups inside the gel is

$$f = c_{\mathrm{PCOO^-}}/c_0 = K_d^g/(K_d^g + c_{\mathrm{H^+}}^g) \tag{A3}$$

where $c_0 \equiv c_{\mathrm{PCOO^-}} + c_{\mathrm{PCOOH}}$. Although c_0 is not precisely known for the poly(acrylic acid) gels under discussion, we adopt a plausible value, c_0 = 0.01 M, that is likely a lower limit. For the qualitative purposes of this discussion, this choice will suffice.

The gel is first equilibrated with a bath containing deionized water with pH 5.7, which implies a proton concentration of $c_{\mathrm{H^+}}^b = 2 \times 10^{-6}$ M. This proton concentration is presumed to arise entirely from the dissociation of adventitious carbonic acid according to the reaction

$$\mathrm{H_2CO_3} \rightleftharpoons \mathrm{HCO_3^-} + \mathrm{H^+} \tag{A4}$$

with equilibrium constant

$$K_d^c = (c_{\mathrm{HCO_3^-}})(c_{\mathrm{H^+}})/(c_{\mathrm{H_2CO_3}}) = 2.5 \times 10^{-4}\ \mathrm{M} \tag{A5}$$

The hydroxide concentration corresponding to $c_{\mathrm{H^+}}^b = 2.0 \times 10^{-6}$ M is $c_{\mathrm{OH^-}}^b = 5 \times 10^{-9}$ M, which is negligible compared to $c_{\mathrm{H^+}}^b$. Consequently, electroneutrality of the bath requires $c_{\mathrm{HCO_3^-}}^b = c_{\mathrm{H^+}}^b - c_{\mathrm{OH^-}}^b \cong 2.0 \times 10^{-6}$ M. Using these results in eq A5 yields $c_{\mathrm{H_2CO_3}}^b = 1.6 \times 10^{-8}$ M. Further use of the equilibrium constant

$$K_h = c_{\mathrm{H_2CO_3}}/c_{\mathrm{CO_2(aq)}} = 1.7 \times 10^{-3} \tag{A6}$$

for the hydration reaction

$$\mathrm{CO_2(aq)} + \mathrm{H_2O} \rightleftharpoons \mathrm{H_2CO_3} \tag{A7}$$

yields $c_{\mathrm{CO_2(aq)}}^b = 9.41 \times 10^{-6}$ M.

When the dilute gel is equilibrated with this bath, which is assumed to be very large, one must have $c_{\mathrm{H_2CO_3}}^g = c_{\mathrm{H_2CO_3}}^b$. Because eq A5 applies in both the bath (b) and the gel (g), one must also have

$$(c_{\mathrm{H^+}}^g)(c_{\mathrm{HCO_3^-}}^g) = (c_{\mathrm{H^+}}^b)(c_{\mathrm{HCO_3^-}}^b) = (2 \times 10^{-6})^2 \tag{A8}$$

Because $c_{\mathrm{H^+}}^g$ will be generally greater than $c_{\mathrm{H^+}}^b$, the $\mathrm{OH^-}$ concentration in the gel again contributes negligibly to the charge balance in the gel, which is then given by

$$c_{\mathrm{H^+}}^g = c_{\mathrm{HCO_3^-}}^g + c_{\mathrm{PCOO^-}} \tag{A9}$$

After solving eq A9 for $c_{\mathrm{HCO_3^-}}^g$, substituting that into eq A8, and using eq A3, there results

$$c_{\mathrm{H^+}}^g = \left(\frac{K_d^g c_{\mathrm{H^+}}^g c_0}{K_d^g + c_{\mathrm{H^+}}^g} + (c_{\mathrm{H^+}}^b)(c_{\mathrm{HCO_3^-}}^b) \right)^{1/2} \tag{A10}$$

For $K_d^g = 10^{-6}$ M and c_0 = 0.01 M (assumed), eq A10 is readily solved by iteration (using $(c_{\mathrm{H^+}}^b)(c_{\mathrm{HCO_3^-}}^b) = 4 \times 10^{-12}$) to yield $c_{\mathrm{H^+}}^g = 1.0 \times 10^{-4}$ M. Use of this value in eq A8 yields $c_{\mathrm{HCO_3^-}}^g = 4 \times 10^{-8}$ M. Inserting both of these values into eq A5 yields $c_{\mathrm{H_2CO_3}}^g = 1.6 \times 10^{-9}$ M, which precisely matches $c_{\mathrm{H_2CO_3}}^b$, as already anticipated. Use of this value in eq A6 yields $c_{\mathrm{CO_2}}^g(\mathrm{aq}) = 9.41 \times 10^{-6}$ M, which precisely matches $c_{\mathrm{CO_2}}^b(\mathrm{aq})$, as also was anticipated.

Although the equilibrium concentrations of neutral species, like $\mathrm{CO_2(aq)}$ and $\mathrm{H_2CO_3}$ are the same in the gel as in the bath, that of a counterion of the gel (e.g., $\mathrm{H^+}$) is greater in the gel ($c_{\mathrm{H^+}}^g = 10^{-4}$ M) than in the bath ($c_{\mathrm{H^+}}^b = 2 \times 10^{-6}$ M), whereas that of a co-ion of the gel (e.g., $\mathrm{HCO_3^-}$) is lower in the gel ($c_{\mathrm{HCO_3^-}}^g = 4 \times 10^{-8}$ M) than in the bath ($c_{\mathrm{HCO_3^-}}^b = 2 \times 10^{-6}$ M). That is the qualitative essence of the Donnan effect. The ionized fraction of poly(acrylic acid) (in the gel) is f = 0.01 under these conditions.

We now consider the same gel in equilibrium with a pH 8.0 solution with the same total carbonate concentration as the pH 5.7 solution discussed above. A pH of 5.7 is typical of deionized water and is attributable to adventitious $\mathrm{CO_2(aq)}$ from the air which can be presumed present in all distilled/deionized water after prolonged exposure to air. We imagine that such a solution was treated quickly with sufficient NaOH to provide a final pH of 8.0, then isolated from further contact with air except for a negligibly small amount of residual air in the container. Consequently, it has the same residual total carbonate as the pH 5.7 bath

$$\begin{aligned} c_C &= c_{\mathrm{HCO_3^-}}^b + c_{\mathrm{H_2CO_3}}^b + c_{\mathrm{CO_2(aq)}}^b \\ &= 2 \times 10^{-6} + 1.6 \times 10^{-8} + 9.41 \times 10^{-6} \\ &= 1.14 \times 10^{-5}\ \mathrm{M} \end{aligned} \tag{A11}$$

After noting that

$$c_{\mathrm{H_2CO_3}}/c_C = 1/(1 + K_d^c/c_{\mathrm{H^+}}^b + 1/K_h) = 3.91 \times 10^{-5}\ \mathrm{M} \tag{A12}$$

we obtain $c_{\mathrm{H_2CO_3}} = 4.45 \times 10^{-10}$ M, $c_{\mathrm{HCO_3^-}}^b = 1.11 \times 10^{-5}$ M, $c_{\mathrm{OH^-}}^b = 10^{-6}$ M, $c_{\mathrm{H^+}}^b = 10^{-8}$ M, $c_{\mathrm{Na^+}}^b = c_{\mathrm{HCO_3^-}}^b + c_{\mathrm{OH^-}}^b = 1.21 \times 10^{-5}$ M, and $c_{\mathrm{CO_2(aq)}} = 2.62 \times 10^{-7}$ M. This solution can be regarded as comprising 1.11×10^{-5} M $\mathrm{NaHCO_3}$ plus 1×10^{-6} M NaOH plus much smaller concentrations of $\mathrm{H_2CO_3}$ and $\mathrm{CO_2(aq)}$.

When the poly(acrylic acid) gel is equilibrated with this pH 8.0 solution, it is found by the same arguments as before that, inside the gel, $c_{\mathrm{H_2CO_3}} = 4.45 \times 10^{-10}$ M, $c_{\mathrm{CO_2(aq)}} = 2.62 \times 10^{-7}$ M, $c_{\mathrm{H^+}}^g = 2.41 \times 10^{-6}$ M (pH 5.62), $c_{\mathrm{OH^-}}^g = 4.15 \times 10^{-9}$ M, $c_{\mathrm{Na^+}}^g = 2.94 \times 10^{-39}$ M, $c_{\mathrm{HCO_3^-}}^g = 4.65 \times 10^{-8}$ M, f = 0.29, and $c_{\mathrm{PCOO^-}}$

dx.doi.org/10.1021/jp302589y | J. Phys. Chem. B 2013, 117, 7653−7674

= 2.93 × 10^{-3} M. The dominant ions in the gel are Na^+ and $PCOO^-$, and their similar concentrations are much greater than when the gel was equilibrated with the pH 5.7 deionized water, for which $c^g_{Na^+} = 0$ and $c_{PCOO^-} = 10^{-4}$ M. In effect, considerable NaOH has entered the gel from the solution and titrated the carboxyl groups to increase the ionized fraction from 0.01 to 0.29. This would produce a substantial deficit of NaOH in the solution near the gel, thereby causing an outward gradient of ln c_{OH^-}, and an outward force on carboxylated microspheres. This prediction matches the observed exclusion of carboxylated microspheres from the poly(acrylic acid) gel.

The pH of the amidinated microsphere suspension is ∼4.0, which is here attributed to added HCl. The acidity in this case drives HCO_3^- to H_2CO_3 and CO_2(aq), so HCO_3^- contributes negligibly to charge balance, and $c^b_{H^+} \cong c^b_{Cl^-} = 10^{-4}$ M. When the same poly(acrylic acid) gel is equilibrated with this solution, the charge balance is

$$c^g_{H^+} = c^g_{PCOO^-} + c^g_{Cl^-} \tag{A13}$$

The Donnan condition is

$$(c^g_{H^+})(c^g_{Cl^-}) = (c^b_{H^+})(c^b_{Cl^-}) = 10^{-8} \tag{A14}$$

and together with eq A13 yields $c^g_{H^+} = 1.41 \times 10^{-4}$ M, $c^g_{Cl^-} = 7.08 \times 10^{-5}$ M, $f = 7.04 \times 10^{-3}$, and $c_{PCOO^-} = 7.04 \times 10^{-5}$ M. Upon going from pre-equilibration with the pH 5.7 deionized water to equilibration with the 10^{-4} M HCl solution, $c^g_{H^+}$ increases from 10^{-4} to 1.41 × 10^{-4}, $c^g_{Cl^-}$ increases from 0 to 7.084 × 10^{-5} M, f decreases from 0.01 to 7.04 × 10^{-3}, and $c^g_{PCOO^-}$ decreases from 10^{-4} to 7.04 × 10^{-5}. It may be concluded that sufficient Cl^- has entered the gel to provide $c_{Cl^-} = 0.708 \times 10^{-4}$ M. A comparable amount of H^+ has entered the gel to raise c_{H^+} by 0.411 × 10^{-4} M and to protonate (1 − 0.704) × 10^{-4} = 0.296 × 10^{-4} M $PCOO^-$ groups, which requires a total amount of protons equivalent to (0.411) × 10^{-4} + (0.296) × 10^{-4} = 0.707 × 10^{-4} M. The amounts of new H^+ and Cl^- that entered the gel are practically identical. It may be concluded that significant HCl is transferred from the solution to the gel. This will produce an HCl deficit in the solution near the gel surface, an outward gradient of ln c_{H^+}, and an outward force on amidinated spheres. This prediction matches the observed exclusion of amidinated spheres from the poly(acrylic acid) gel.

AUTHOR INFORMATION

Corresponding Author

*Phone: 206-543-6681. Fax: 206-685-8665. E-mail: schurr@chem.washington.edu.

Notes

The authors declare no competing financial interest.

REFERENCES

(1) Zheng, J.-M.; Pollack, G. H. Long-Range Forces Extending from Polymer-Gel Surfaces. *Phys. Rev. E* **2003**, *68*, 031408-1−031408-7.

(2) Zheng, J.-M.; Chin, W. C.; Khijniak, E.; Khijniak, E., Jr.; Pollack, G. H. Surfaces and Interfacial Water: Evidence That Hydrophilic Surfaces Have Long-Range Impact. *Adv. Colloid Interface Sci.* **2006**, *127*, 19−27.

(3) Zheng, J.-M.; Pollack, G. H. Solute Exclusion and Potential Distribution near Hydrophilic Surfaces. In *Water and the Cell*; Pollack, G. H., Cameron, I. L., Wheatley, D. N., Eds.; Springer: The Netherlands, 2006; pp 165−174.

(4) Zhao, Q.; Zheng, J.-M.; Chai, B.; Pollack, G. H. Unexpected Effect of Light on Colloidal Crystal Spacing. *Langmuir* **2008**, *24*, 1750−1755.

(5) Zheng, J.-M.; Wexler, A.; Pollack, G. H. Effects of Buffers on Aqueous Solute-Exclusion Zones around Ion-Exchange Resins. *J. Colloid Interface Sci.* **2009**, *332*, 511−514.

(6) Nagornyak, E.; Yoo, H.; Pollack, G. H. Mechanism of Attraction between Like-Charged Particles in Aqueous Solution. *Soft Matter* **2009**, *5*, 3850−3857.

(7) Chai, B.; Yoo, H.; Pollack, G. H. Effect of Radiant Energy on Near-Surface Water. *J. Phys. Chem. B* **2009**, *113*, 13953−13958.

(8) Pollack, G. H.; Figueroa, X.; Zhao, Q. Molecules, Water, and Radiant Energy: New Clues for the Origin of Life. *Int. J. Mol. Sci.* **2009**, *10*, 1419−1429.

(9) Chai, B.; Pollack, G. H. Solute-Free Interfacial Zones in Polar Liquids. *J. Phys. Chem. B* **2010**, *114*, 5371−5375.

(10) Chai, B.; Zheng, J.-M.; Zhao, Q.; Pollack, G. H. Spectroscopic Studies of Solutes in Aqueous Solution. *J. Phys. Chem. A* **2008**, *112*, 2242−2247.

(11) Schurr, J. M.; Fujimoto, B. S.; Huynh, L.; Chiu, D. T. A Theory of Macromolecular Chemotaxis. *J. Phys. Chem. B* **2013**, DOI: 10.1021/jp302587d.

(12) Schantz, E. J.; Lauffer, M. A. Diffusion Measurements in Agar Gel. *Biochemistry* **1962**, *1*, 658−663.

(13) Aragon, S.; Hahn, D. Precise Boundary Element Computation of Protein Transport Properties: Diffusion Tensors, Specific Volume, and Hydration. *Biophys. J.* **2006**, *91*, 1591−1603.

(14) Watanabe, K.; Zellikoff, M. Absorption Coefficients of Water Vapor in the Vacuum Ultraviolet. *J. Opt. Soc. Am.* **1953**, *43*, 753−754.

(15) Segelstein, D. J. The Complex Refractive Index of Water. M.S. Thesis, University of Missouri at Kansas City, 1981.

(16) Warren, S. G. Optical Constants of Ice from the Ultraviolet to the Microwave. *Appl. Opt.* **1984**, *23*, 1206−1225.

(17) Sharp, K. A.; Friedman, R.; Misra, V.; Hecht, J.; Honig, B. Salt Effects on Polyelectrolyte-Ligand Binding. Comparison of Poisson-Boltzmann and Limiting Law Counterion Binding Models. *Biopolymers* **1995**, *36*, 245−262.

(18) Diehl, H.; Markuszewski, R. Studies on Fluorescein. 7. The Fluorescence of Fluorescein as a Function of pH. *Talanta* **1989**, *36*, 416−418.

(19) Sha, Y.; Chen, H.; Yin, Y.; Tu, S..; Ye, L.; Zheng, Y. Characteristics of the Marangoni Convection Induced in Initial Quiescent Water. *Ind. Eng. Chem. Res.* **2010**, *49*, 8770−8777.

(20) Bertie, J. E.; Lan, Z. Infrared Intensities of Liquids .20. The Intensity of the OH Stretching Band of Liquid Water Revisited, and the Best Current Values of the Optical Constants of H_2O(l) at 25 degrees C between 15,000 and 1 cm^{-1}. *Appl. Spectrosc.* **1996**, *50*, 1047−1057.

(21) Zhao, Q.; Ovchinnikova, K.; Chai, B.; Yoo, H.; Magula, J.; Pollack, G. H. Role of Proton Gradients in the Mechanism of Osmosis. *J. Phys. Chem. B* **2009**, *113*, 10708−10714.

(22) Zhao, Q.; Coult, J.; Pollack, G. H. Long-Range Attraction in Aqueous Colloidal Suspensions. *Proc. SPIE* **2010**, *7376*, 73761c-1−73761c-13.

(23) Stygar, W. A.; Wagoner, T. C.; Ives, H. C.; Wallace, Z. R.; Anaya, V.; Corley, J. P.; Cunco, M. E.; Harjes, H. C.; Lott, J. A.; Mowrer, G. R.; et al. Water-Dielectric-Breakdown Relation for the Design of Large-Area Multimegavolt Pulsed-Power Systems. *Phys. Rev. Spec. Top.—Accel. Beams* **2006**, *9*, 070401-1−070401-10.

(24) Ovchinnikova, K.; Pollack, G. H. Can Water Store Charge? *Langmuir* **2009**, *25*, 542−547.

(25) Corti, H. R.; Colussi, A. J. Do Concentration Cells Store Charge in Water? Comment on Can Water Store Charge? *Langmuir* **2009**, *25*, 6587−6589.

(26) Corti, H. R.; Colussi, A. J. Response to Reply to Comment on Can Water Store Charge? *Langmuir* **2009**, *25*, 11203.

(27) Ovchinnikova, K.; Pollack, G. H. Reply to Comment on Can Water Store Charge? *Langmuir* **2009**, *25*, 11202.

(28) Schurr, J. M. Theory of Quasielastic Light Scattering from Chemically Reactive Ionic Solutions. *J. Phys. Chem.* **1969**, *73*, 2820−2828.

(29) Lin, S.-C.; Lee, W.-I.; Schurr, J. M. Brownian Motion of Highly Charged Poly(L-lysine). Effects of Salt and Polyion Concentration. *Biopolymers* **1978**, *17*, 1041−1064.
(30) Schurr, J. M. Dynamic Light Scattering and Mutual Diffusion in Non-Ideal Systems. One-Component and Multicomponent Spherical Solutes. *Chem. Phys.* **1987**, *111*, 55−86.
(31) Schurr, J. M.; Schmitz, K. S. Dynamic Light Scattering Studies of Biopolymers. Effects of Charge, Shape, and Flexibility. *Annu. Rev. Phys. Chem.* **1986**, *37*, 271−305.
(32) Campion, J. J. Alternate Approach to Liquid Junction Potentials. *J. Chem. Educ.* **1972**, *49*, 827−828.
(33) Samec, Z.; Trojánek, A.; Samcová, E. Evaluation of Ion-Transport Parameters in a Nafion Membrane from Ion-Exchange Measurements. *J. Phys. Chem.* **1994**, *98*, 6352−6358.
(34) Yoo, H.; Paranji, R.; Pollack, G. H. Impact of Hydrophilic Surfaces on Interfacial Water Dynamics Probed with NMR Spectroscopy. *J. Phys. Chem. Lett.* **2011**, *2*, 532−536.
(35) Mitchell, H. J.; Salvaggio, C. Effects of Surface and Internal Water on the Emissive Spectral Signatures of Materials. *Proc. SPIE* **2003**, *5093*, 195−205.
(36) Shaw, J. A.; Marston, C. *Opt. Express* **2000**, *7*, 375−380.
(37) Fatkullin, R. G.; Khusainov, B. G. Determination of Meniscus Height. *Ismer. Tekh.* **1979**, *10*, 48−50.
(38) Edwards, M.; Benjamin, M. M.; Ryan, J. N. Role of Organic Acidity in Sorption of Natural Organic Matter (NOM) to Oxide Surfaces. *Colloids Surf., A* **1996**, *107*, 297−307.